Tsunami hazard in the Caribbean: Regional exposure derived from credible worst case scenarios

C.B. Harbitz, S. Glimsdal, Sara Bazin, N. Zamora, F. Løvholt, H. Bungum, H. Smebye, P. Gauer, O. Kjekstad

Tsunami hazard in the Caribbean: Regional exposure derived from credible worst case scenarios

C. B. Harbitz[1,2*] , S. Glimsdal[1,2] , S. Bazin[1,2,3], N. Zamora[4], F. Løvholt[1,2], H. Bungum[5,2], H. Smebye[1,2], P. Gauer[1,2], O. Kjekstad[1,2]

1 Norwegian Geotechnical Institute (NGI), Norway; 2 International Centre for Geohazards (ICG), Norway[*]; 3 Previously at Institut de Physique du Globe de Paris, France; 4 Research collaboration with University of Costa Rica, previously at ICG; 5 NORSAR, Norway.

Abstract

The present study documents a high tsunami hazard in the Caribbean region, with several thousands of lives lost in tsunamis and associated earthquakes since the XIXth century. Since then, the coastal population of the Caribbean and the Central West Atlantic region has grown significantly and is still growing. Understanding this hazard is therefore essential for the development of efficient mitigation measures. To this end we report a regional tsunami exposure assessment based on potential and credible seismic and non-seismic tsunamigenic sources. Regional tsunami databases have been compiled and reviewed, and on this basis five main scenarios have been selected to estimate the exposure. The scenarios comprise two M_w8 earthquake tsunamis (north of Hispaniola and east of Lesser Antilles), two subaerial/submarine volcano flank collapse tsunamis (Montserrat and St Lucia), and one tsunami resulting from a landslide on the flanks of the Kick'em Jenny submarine volcano (north of Grenada). Offshore tsunami water surface elevations as well as maximum water level distributions along the shore lines are computed and discussed for each of the scenarios. The number of exposed people has been estimated in each case, together with a summary of the tsunami exposure for the earthquake and the landslide tsunami scenarios. For the earthquake scenarios, the highest tsunami exposure relative to the population is found for Guadeloupe (6.5%) and Antigua (7.5%), while St. Lucia (4.5%) and Antigua (5%)

[*] Corresponding author, C. B. Harbitz, NGI, P.O. Box 3930, Ullevål stadion, N-0806 Oslo, Norway. Phone: +4722023000. Fax +47 22230448. Email: ch@ngi.no.

has been found to have the highest tsunami exposure relative to the population for the landslide scenarios. Such high exposure levels clearly warrant more attention on dedicated mitigation measures in the Caribbean region.

Keywords : Caribbean, tsunami, earthquake, volcano, landslide, run-up, exposure

1 Introduction

Tsunami hazard is more difficult to assess than earthquake hazard for two main reasons, firstly that the tsunamigenic processes are diverse (earthquakes, volcanoes, landslides, or some combination of these) and secondly that the relation between the energy released in the process (such as the earthquake magnitude) and the size of the tsunami generally is quite complex, and non-linear. Moreover, a problem that tsunami hazard shares with earthquake hazard is the extreme scaling laws, demonstrated by the way the consequences (the risk) increase with decreasing occurrence probabilities. What this means in real life is that the most severe earthquake and tsunami disasters are very rare and have scaling characteristics such that they saturate only at a very high level (as compared for instance to winds and ocean waves) and that they therefore are difficult to predict when based on empirical data that cover only a few hundred years, even though paleoseismic and paleotsunamic studies have now significantly increased the time frames here. For these (and other) reasons, probabilistic assessment of tsunami hazard is still at an early stage of development (Løvholt et al. 2011), and we find therefore that scenario based assessments represent a more viable approach, as used in this study.

The Caribbean is one of the most highly exposed regions of the world with respect to natural hazards, as seen recently by the January 2010 Haiti earthquake and tsunami (Calais et al. 2010; Hornbach et al. 2010; see also ISDR 2009). Climatic hazards such as strong winds and heavy rains, storms and hurricanes frequently give rise to landslides, sediment flows, and water floods. Earthquakes and volcanic activity in the eastern Caribbean are also significant in addition to the relatively high risk levels for coastal flooding, including tsunami risk. In fact, one out of seven tsunamis worldwide is found in the Caribbean Sea (O'Loughlin and Lander 2003). With few exceptions, the capabilities in the region to deal with these hazards in terms of efficient preventive measures have so far been limited (IOC 2006). This is largely a

result of limited technological and human resources, combined with the fact that the region comprises a number of small autonomous states with limited collaboration and integration of capabilities. Experience from most countries exposed to natural disasters is that efforts to build awareness and improve preparedness are crucial in mitigating the large consequences of natural hazards.

This paper presents a study of regional tsunami hazard and related exposure in the Caribbean region, including potential seismic and non-seismic tsunamigenic sources. The paper contains calculations demonstrating a methodology that could easily be expanded into a more comprehensive tsunami hazard and exposure assessment. The regional tsunami risk is assessed as the sum of the effects from a number of scenarios that may affect the various elements at risk. As already mentioned, the tsunami risk is often dominated by large scale 'credible worst case scenarios' (Nadim and Glade, 2006), and the scenarios developed in this paper clearly fall into this category. However, since the scenarios cover only the presumed most important of the potential scenarios, they do not represent the complete tsunami risk. Further applications of the tsunami simulations in a more local and detailed way, with tsunami vulnerability and risk analysis for Bridgetown, Barbados, are presented by NGI (2009a).

2 Geodynamics and potential tsunami sources in the Caribbean region

In the Caribbean region, both earthquakes and non-seismic sources (volcanic eruptions, flank collapses, and submarine landslides) are known to have caused a large number of tsunamis, many of them destructive. Hence, both seismic, volcanic, and landslide activity must be understood for a balanced combination of credible worst case tsunami scenarios and for disaster risk reduction.

2.1 Seismic activity

The Caribbean Plate is bounded to the east by the Lesser Antilles subduction zone and to the west by the Central America subduction zone (Figure 1). The North American and South American plates dip beneath the Caribbean plate at a rate of about 2 cm/yr in a WSW direction along the Lesser Antilles Trench (DeMets et al. 2000; Mann et al. 2002). As a consequence, the Eastern Caribbean is prone to a moderate to large seismic hazard. Three kinds of damaging seismicity can be distinguished in the arc (Stein et al.

1982), firstly, the seismicity directly related to the subduction at the plate interface, secondly, the seismicity within the subducting slab at greater depth, and thirdly, the seismicity occurring within the Caribbean plate.

The largest historical earthquake in the region occurred in 1843 between Guadeloupe and Antigua (geographical names are presented in Figure 2), with a magnitude of 7.5 to 8 (Bernard and Lambert 1988). Since the historical seismicity in this region covers only three and a half centuries, and with variable quality, it is difficult on this basis to estimate the recurrence time of strong events and also their magnitudes. The geometries of the subduction processes in the Caribbean are also quite complex, so it is difficult also on this basis to estimate the potentials. Using the instrumental seismicity available since 1950 in the Lesser Antilles, several authors have described a variable dip angle (from 30° to 60° dip) of the slab along the main arc (Dorel 1981; Girardin and Gaulon 1983; Wadge and Shepherd 1984; Girardin et al. 1991; Feuillet et al. 2002). However, according to Bengoubou-Valerius et al. (2006), with more accurate earthquake locations there is no significant dip variation from north to south and a constant 50° dip angle fits the Wadati-Benioff plane quite well. In general, the subduction rate (the downgoing slab velocity) often tends to increase with the age of the subducted plate due to the density of old oceanic lithosphere (Carlson and Raskin 1983). In the Lesser Antilles, however, the subduction is slow (the rate of convergence is 2cm/yr according to DeMets et al. 2000), while the subducting lithosphere is old (80-85 Ma according to Müller et al. 1997), which is what Ruff and Kanamori (1982) showed in their classical paper to be important criteria for limiting the maximum magnitude. However, the 2004 Sumatra event violated significantly the rule that only young plates with a fast subduction can create megathrust earthquakes, so apparently the Ruff-Kanamori paradigm is too simple. It has also been suggested (Ruff, 1989) that the existence of trench sediments could explain part of the remaining variance in maximum earthquake size, which is interesting here since the southern part of the Lesser Antilles Trench is buried by a large wedge of sediments forming the Barbados accretionary prism (Bengoubou-Valerius et al. 2006). However, a close examination of these and other criteria made Stein and Okal (2007) conclude that the strongest one was possibly age in itself, since no mega-earthquakes (e.g. larger than M_w9.0) are known to have occurred in a subducting lithosphere older than 90 Ma. Even so, it is worth keeping in mind that tsunamis driven by sub-mega earthquakes can also be highly hazardous (Løvholt et al. 2006).

The strike-slip motions relative to the North and South American plates occurs along two major fault zones (Calais et al. 1998; see also Figure 1): the northern plate boundary (Hispaniola and Puerto Rico) dominated by the Enriquillo and Septentrional faults, and the southern plate boundary (Venezuela) dominated bythe El Pilar fault. The type of seismicity associated with strike-slip faulting is shallow and can be damaging, as demonstrated by the 2010 Haiti earthquake. The tsunamigenic potentials of earthquakes are tied to the focal mechanism as the tsunami generation implies a significant vertical displacement (Tanioka and Satake 1996; Hebert et al. 2005); thrust events in subduction zones are therefore generally the most tsunamigenic ones. Grilli et al. (2010) present numerical simulations of both near- and far-field impact of tsunamis generated in the Puerto Rico trench, revealing run-up heights of about 20 m along the northern shore of Puerto Rico for a M_w9.1 source. However, faulting mechanisms are complex in the Caribbean region and do not always reflect only the first order plate motions; for instance, oblique motions at the tip of a strike-slip fault could also produce vertical dislocations. In addition, pure strike-slip earthquakes could trigger submarine landslides that generate tsunamis. A more comprehensive review of the large scale tectonics of the region and of potential seismic sources for tsunamis is presented by NORSAR (NGI 2009b).

The Lesser Antilles volcanic arc has been built up by the subduction of the northern and southern American plates under the Caribbean plate (Molnar and Sykes 1969). It has a curved shape and extends from 12°N to 18°N latitude. North of the island of Martinique, the Lesser Antilles arc is composed of an outer arc, made of Plio-Quaternary coral reef platforms, and of a recent upper Miocene inner volcanic arc. Active volcanoes are located in the western branch of the island chain, with twelve Holocene active volcanoes in the ten major islands of the younger arc. Catastrophic flank collapses are quite frequent for these volcanoes (Boudon et al. 2007).

2.2 Volcanic activity, flank collapses, and landslides

In Guadeloupe, the Grande Découverte-Soufrière composite volcano has experienced at least 12 flank collapse events over the last 50 ka (Komorowski et al. 2002; 2005). During the last 8500 years, 8 small flank-collapse events with volumes of 0.1-0.3 km^3 are known, and some of them reached the Caribbean Sea (Le Friant et al. 2006). The Caracasbai in Curaçao, Netherlands Antilles, is also the result of a huge

slide. With the use of echosounding, a limestone block of about 150 million m^3 has been identified. The block separated from the south-western part of the island and fell into the sea, displacing around 700 million m^3 of globigerina ooze about 5-10 ka BP (de Buisonje and Zonneveld 1976).

Kick'em Jenny is an active growing submarine volcano located 8 km off the northern side of the island of Grenada. According to Pararas-Carayannis (2004) submarine explosive eruptions would be expected to generate tsunamis as a series of smaller events over more than 24 hours. The wave periods and wave lengths will probably be short, however, and wave height will therefore decay rapidly with distance. Based on the pattern of Kick'em Jenny's eruptive activity, a present 'worst case tsunami scenario' would be a repeat of the 1939 event, but with the shallower depth of the present summit. Such a large and violent eruption can be expected to generate waves with a run-up height of 3 m in Northern Grenada and the Grenadines, and as much as 1-2 m along the west coast of the Barbados, Trinidad, and Saint Vincent. The wave heights along the nearest coastline of northern Bonaire, Netherlands Antilles, and Venezuela may be up to 1 m (Pararas-Carayannis, 2004).

Gisler et al. (2006b) demonstrated by 2D numerical simulations of explosive eruptions that a medium scenario for this volcano could generate a wave with a height of 130 m at a distance of 3 km from the source and a height of 21 m at 10 km distance, comparable to an explosion of about 20,000 kT. However, in the simulations the submerged top was only 100 m below the water surface, thus significantly shallower than the true cone summit. They also state that the water depth above the volcano summit is now 190 m, and is not significantly diminishing. Hence, the water pressure confines the explosive effects, and the coupling of the explosive energy to wave energy is inefficient compared to slower mechanisms such as landslides (only a few percent of the explosive source energy is transferred). Gisler et al. (2006b) therefore concluded that there is presently a modest danger related to explosive eruptions except for gases and missiles threatening shipping, and that the tsunami danger from Kick'em Jenny is larger for a slope failure similar to that which caused the horse-shoe shaped cleft in which the volcano currently nestles. The debris flows of Kick'em Jenny were described by Sigurdsson et al. (2006). These flows extend from the western side of the submarine volcano for about 15 km to maybe 30 km to the west into the Grenada Basin (west of Grenada) with a thickness of tens to hundreds of meters. A conservative estimate of the volume of the smaller debris flow deposits is about 10 km^3. It is possible that hydromagmatic

explosions associated with future eruptions could result in greater flank instability and maybe also slow the rate of growth of the volcano (Pararas-Carayannis 2004).

Using high-resolution bathymetric data, Deplus et al. (2001) mapped large-scale debris flow deposits on the seafloor surrounding several active volcanoes. These flow deposits most likely represent catastrophic events also generating huge tsunamis. Three smaller debris flow deposits of about 20-120 km^2 were identified on the lower submarine flanks of the Soufriere Hills volcano in Montserrat. They are characterized by mega-blocks 100-400 m across and 20-40 m high in addition to smaller debris flow blocks, and they extend to about 15 km from the shoreline. The age of the debris flows is probably less than 100-200 ka (Deplus et al. 2001). The major English's Crater event about 4000 years BP involved a volume of 0.5 km^3 (Le Friant et al. 2004). Off the southern parts of Montserrat some of the observed deposits could have originated either as a submarine flank failure or as an older subaerial flank collapse that subsequently have been buried by the South Soufriere Hills volcano. Large-scale debris flow deposits are also identified west of the active volcanoes of Martinique, Dominique, and Saint Lucia. Off Martinique and Saint Lucia, the deposits are found at the opening of flat-floored channels in the continuity of the horseshoe-shaped structures of Mt Pelée (Martinique) and Qualibou (Saint Lucia). The deposits cover areas of about 3500 km^2 off Dominica, 800 km^2 off Martinique, and 2000 km^2 off Saint Lucia, with terrain covered by mega-blocks over 1100 km^2, 60 km^2 and 300 km^2, respectively. The run-out distances for the debris flow blocks are about 90 km for Dominica, 60 km for Martinique, and 75 km for Saint Lucia. The deposits probably resulted from several flank collapse events for each volcano, but the long run-out distances demonstrate that they were produced by major events. The age of the debris flows is probably also here less than 100-200 ka (Deplus et al. 2001).

Many forested volcanic islands of the Lesser Antilles have highly eroded oversteepened coastal cliffs that can cause large landslides, and therefore present significant tsunami hazards. Due to surveying difficulties these areas have not been properly studied to date, but new remote sensing techniques could provide appropriate methods of investigation (Teeuw et al. 2009).

Recent geomorphological landslide data obtained by marine geophysical surveys have also given interesting results for studying possible tsunami sources; for instance, the ones located in the Puerto

Rico region are described by ten Brink et al. (2004). The Loiza amphitheatre (and a 15 km long fissure) and the Arecibo amphitheatre (50 km wide escarpment), both on the southern side of the Puerto Rico Trench, the northern side of the Puerto Rico trench, and the Mona rift (between Puerto Rico and Hispaniola) were all interpreted as failures capable of generating tsunamis. The Loiza debris extends for 40 km with a thickness of 200 m. From 160 landslides described in the area only 9 are supposed to have volumes of more than 5 km^3 (ten Brink et al. 2006a), and only these could have caused tsunami run-ups higher than 2.5 m. The numerical tsunami modelling by ten Brink et al. (2006a) predicted a maximum tsunami run-up of approximately 16 m on the northern coast of Puerto Rico. This region may generate significant tsunamis mainly towards the coast of Puerto Rico, Virgin Islands, and Dominican Republic. The conditions of the Mona Canyon and its secondary canyons with their steep slopes may possibly generate submarine landslides. Quantifying this hazard is difficult, however, due to scarce historical information (Moya and Mercado 2006).

3 Past tsunami events

3.1 Historical tsunamis database

Historical Caribbean tsunamis have been studied by several researchers (e.g. McCann 2006), but with only some of them going back to original data and analyzing data from the many scattered archives in this region (Zahibo and Pelinovsky 2001; BRGM 2009; Nikolkina et al. 2010). We have compiled a new historical tsunami database for the Caribbean Sea largely based on the reports from the NOAA National Geophysical Data Center (NOAA/NGDC 2008) and the Novosibirsk Tsunami Laboratory (NTL 2002), which in turn are based on tsunami catalogues compiled by O'Loughlin and Lander (2003), Mercado-Irizarry and Liu (2006), and Shepherd et al. (1995). For many of the events we have updated the source information based on recent updates of earthquake locations, focal depths, magnitudes, and tsunami observations (Engdahl and Villaseñor 2002; Engdahl et al. 2007; Villaseñor and Engdahl 2007; BRGM 2009). This reassessment has led to some significant adjustments. In our updated database (available in the Appendix), a total of 85 tsunamis are documented, comprising only definite, probable, or questionable events. Events labelled unlikely or erroneous have been removed. Some data have also been removed (by us) after a careful inspection of the literature sources.

The first reported tsunami in the new database occurred in Venezuela in 1498, while the first tsunami with definite tectonic origin occurred in 1530 in Cumanà, Venezuela. The database ends with the tsunami caused by the eruption of Soufriere Hills of Montserrat in 2006. Although unlikely, we cannot exclude the possibility that a significant historical tsunami may have escaped the above-mentioned catalogues during the past five centuries. We find that 17 of the 85 tsunamis report fatalities and that more than 15 000 people have perished due to tsunamis since 1498, which means that the number of tsunami casualties in the Caribbean exceeds that of the U.S. West Coast, Hawaii, and Alaska combined (ten Brink et al. 2005). A total of 74% of the listed tsunamis were caused by earthquakes, 14% by volcanoes, 7% by landslides, and only 5% are of unknown origin (Figure 3).

Both the NOAA/NGDC (2008) and the NTL (2002) databases include a mix of run-up heights and highest reported wave heights (H). It is assumed that most of these refer to the run-up heights and we have kept both these values together under maximum wave level in our database. In addition tsunamis with intensity $I = \log_2(\sqrt{2}H)$ (Soloviev and Go 1984) or tsunami magnitude $M_I = \log_2(H)$ (Iida et al. 1967) were referred to in the original databases, and we applied the *H* value derived from these expressions as maximum water level in our database. The reported tsunami heights and fatalities with respect to source types are presented in Figure 4. The earthquake magnitude included in the original data was either unspecified or reported as the surface wave magnitude M_S or the moment magnitude M_W. We kept all original information in our database, presented the M_S or M_W values for the various events together, and favoured M_w when both values were available for the same event.

3.2 Historical seismic tsunami sources

According to O'Loughlin and Lander (2003), only two trans-oceanic tsunamis have been reported in the Caribbean Sea, the first of which resulted from the November 1, 1755 Lisbon earthquake (Baptista et al. 1998; 2003). The tsunami wave had an amplitude of up to 20 meters at Lisbon and along the African and south European coasts, and of 6.4 meters at the island of Saba in the Lesser Antilles (Baptista et al. 2003). A second trans-oceanic tsunami was recorded after the earthquake on the Iberian coast on March 31, 1761, causing considerable flux and reflux in Barbados, with a run up height of about 1.2 m (Lander and Whiteside 1997; O'Loughlin and Lander 2003).

Altogether 62 of the 85 reported Caribbean tsunamis (Figure 4) are of regional seismic origin, and they occur in different tectonic contexts, as subduction and strike-slip events at the plate boundaries, and as intraplate events. The highest tsunami wave occurred on November 18, 1867, after a strong M_S 7.5 earthquake in the Virgin Islands. This severe tsunami travelled across all the Lesser Antilles islands. There is still disagreement about the maximum run-up heights (8.8 m or 10 m in Table 1). The 1867 Virgin Island tsunami is simulated numerically by Zahibo et al. (2008) and their results are in close agreement with the observations in many islands of the Caribbean Sea except for the island of Guadeloupe where a run-up height of 18.3 m was originally reported, however recently reduced to 10 m (NOAA/NGDC 2011).The reduction is based on inspection of the site and investigation of historical documents by Zahibo and Pelinovsky (2001), who stated that a run-up height up to 10 m seems more realistic in Deshaies, perhaps as small as 5 m (Zahibo et al. 2003). Barkan and ten Brink (2010) also performed simulations of the 1867 Virgin Island tsunami and found that the epicentre location was along the upper part of the northern wall of the Virgin Islands basin, and not in the Virgin Islands basin, as commonly assumed.

3.3 Historical non-seismic tsunami sources

A thorough literature survey on non-seismic tsunamigenic sources in the region is presented by NGI (2009c).

Volcanic eruptions and flank collapses

Eruptions accompanied by collapsed lava domes, flank failures, pyroclastic flows, lahars, and debris flows can all generate tsunamis (e.g., Brown et al. 1977). The eruption on Montserrat on December 26, 1997, was followed by a pyroclastic flow that reached the ocean and caused 3 m waves and 80 m of inundation (Heinrich et al. 1998; Pararas-Carayannis, 2004). The previous 1995 eruption did not generate a tsunami, but probably weakened the Soufriere Hills' flanks and thus caused the flank failures associated with the eruptions in 1997, 1999, 2003, and 2006, which did generate tsunamis. The July 12, 2003 tsunami following a major collapse of the lava dome and a pyroclastic flow that reached the sea was reported to about 4 m on Montserrat and about 0.5-1 m on Guadeloupe (Pelinovsky et al. 2004; Poisson and

Pedreros 2010). On May 20, 2006, another tsunami of volcanic origin reached Montserrat with a height of 1 m.

There are reports of a tsunami on Martinique in 1767, but the height of the waves and their origin are uncertain. Two important events related to the Mt Pelée, Martinique eruptions took place in 1902. On May 5 that year Mt Pelée began erupting and produced destructive lahars with speeds of about 100 km/hour. The lahars continued into the sea and generated a 4-5 m tsunami, affecting the areas of St Pierre. Based on numerical simulations of the event, Poisson and Pedreros (2010) argue that the tsunami was generated by three successive lahars rather than a single instantaneous source. A second event occurred on May 8, 1902. The day before, sea disturbances of up to 1 m were reported in the harbours of Grenada, Barbados, and Saint Lucia (NOAA/NGDC 2008). These disturbances were possibly caused by the flank failure of Mt Pelée or by pyroclastic flows reaching the sea from the eruption of the Soufrière volcano on Saint Vincent.

Kick'em Jenny's first recorded eruption occurred in 1939, causing a series of tsunami-like waves with amplitudes of about 2 m in the Grenadines and the Grenada Island. More eruptions occurred in 1943, 1953, 1965, 1966, 1972, 1977, 1988 and 1990, but with no tsunami triggering. Two more tsunami events, although with scarce information, occurred on February 17, 1843, in Antigua and on November 3, 1911, in Trinidad. Both are supposed to have a volcanic origin.

Submarine landslides

Tsunamis that are generated by submarine landslides are often associated with earthquakes (O'Loughlin and Lander 2003), and they can cause considerable impacts even on distant shores (Masson et al. 2006; Harbitz et al. 2007). Pararas-Carayannis (2004) mentions that a fairly unknown event on May 7, 1902 cut the submarine communication cables from the island of Martinique to the outside world, and that the cable failures could have been caused by an underwater debris avalanche.

4 Tsunami modelling approach

4.1 Seismic sources

The earthquake rupture is generally a rapid process, and the main tsunami generation is therefore most often completed within a few minutes. Hence, the initial wave mimics the seabed elevation with a few modifications. For the purpose of tsunami modelling the co-seismic dislocations are normally converted to seabed displacements through a standard analytical formula (Okada 1985). The input to this formula is the position, width and length of fault, as well as dip-slip, strike-slip, focal depth, and dip angle. The seabed displacement is then transferred to the sea surface. Finally, a two-dimensional (2D) solution of the Laplace equation established by matched asymptotics is employed to smooth out sea surface discontinuities above the fault line (Pedersen 2001). The sea surface elevation is finally applied as an initial condition for the tsunami propagation model with the water initially at rest. For further details on design of the seismic scenarios, see Løvholt et al. (in review).

4.2 Landslide sources

Tsunamis generated by landslides (submarine and subaerial) are caused mainly by the volume displacements of the flowing masses. In this process, the water is elevated above the front of the landslide, whereas a water depression is found above the tail of the landslide. Submarine landslides are often clearly sub-critical, i.e. the Froude number (defined as the ratio of the landslide speed to the linear hydrostatic wave speed) is much less than one. This implies that the wave will normally run away from the wave-generating landslide, limiting the build-up of the wave. However, critical effects (i.e. Froude number close to one) are often important for tsunamis generated by volcanic flank collapses or rock slides, where the sliding masses impact shallow water with high velocities.

In our modelling of the landslide scenarios (subaerial and submarine), the landslide is simplified as a flexible box with a prescribed velocity progression. The landslide box is rounded to avoid numerical noise due to sharp edges. The dimensions and configuration of the landslides are determined from the literature on previous events, from studies of the mapped deposits, and by visual reconstruction of the

landslide scar topography. The impact velocity is determined by analytical energy considerations and from literature on simulations of pyroclastic flows (e.g., Heinrich et al. 1998; Le Friant et al. 2006). The submarine run-out distance is determined by the mapped deposits from previous events and by statistics of fall height to run-out distance ratios versus volumes (De Blasio et al. 2006). This returns run-out distances clearly shorter than those reported for debris flow blocks in Section 2.2, which is reasonable as such blocks most often reach longer than the full debris flow (that the block might originate from). Further, these blocks do not contribute much to the tsunami generation. In the model, the landslide follows a straight line (note that the initial phase of the landslide progression principally determines the characteristics of the generated waves, see e.g. Løvholt et al. 2005). The seabed displacement caused by the landslide is calculated and applied as input to the tsunami propagation model. From previous experience, the prescribed model for the landslide configuration and progression gives reasonable results for the tsunami propagation, in light of the overall uncertainty (landslide parameters, etc.). For further details on representation of and tsunami generation by landslides, see Harbitz (1992) and Løvholt et al. (2005).

4.3 Tsunami propagation

For the tsunami propagation, we apply the depth-averaged three-dimensional tsunami model (a model with two horizontal dimensions, 2HD) GloBouss (Pedersen and Løvholt 2008; Løvholt et al. 2008; Løvholt el al. 2010). This model is based on the Boussinesq equations including higher order dispersion terms, Coriolis terms, and numerical hydrostatic correction terms. Boussinesq models capture both the effect of non-linearity (steepening of the wave front in shallower water) and dispersion (wavelength dependent wave speed). GloBouss further includes possibilities to utilize both Cartesian and geographical coordinates. Landslides are included through sink-source (velocity) distributions of the seabed deformations as function of time, whereas earthquake generated tsunamis are included as initial conditions for the sea surface (see above). The bathymetric data applied for this study is based on the General Bathymetric Chart of the Oceans (GEBCO 2008) 1’ grid.

4.4 Alongshore distribution of the maximum water levels

To find an estimate of the tsunami impact on land, the corresponding run-up or alternatively the shoreline water levels along all the affected coastlines must be calculated. For a regional study including hundreds of locations and hundreds to thousands of kilometres of shoreline, it is too time consuming to perform refined numerical inundation investigations for all scenarios for each of the locations. Instead a faster, but still reliable procedure to transfer the offshore tsunami surface elevation to the shoreline water levels was used, determining the amplification factors from the parameters describing the incoming wave, bathymetric slope, etc.

To find these factors, a series of simulations with different tsunami characteristics (leading depression/peak, wave period) were performed on a set of different idealized bathymetric profiles (Løvholt et al. 2011). These simulations serve as a database for the amplification factors between the offshore surface elevation and the onshore water level. Two different numerical models have been used to determine the amplification factors. Both models are of the Boussinesq type, but in this context the models are applied in a linear hydrostatic mode. Primarily, a tsunami propagation model in one horizontal dimension (1HD) for simulating waves along vertical transects is used (Vanneste et al. 2010), whereas the 2HD model GloBouss described above is used for determination of the amplification factors at smaller islands. The inclusion of a 2HD model for determining the amplification of the tsunami at smaller islands are needed due to three dimensional effects not captured along transects.

Outside each location to be investigated a 'control point' was put at a water depth of 50 m to measure the surface elevation (time series). The maximum surface elevation measured at the point was extracted and the shape of the leading wave (depression or peak) and the wave period were determined. By visual inspection of the bathymetry (from deep water to the shoreline), it is determined what idealized profile that matches the best way. The amplification factor for the given set of parameters is then extracted from the database. Finally, the maximum surface elevation measured at the control point is multiplied by the amplification factor to find the maximum shoreline water level. For a detailed description of this methodology, see NGI (2009c) and Løvholt et al. (2011). Effects such as refraction and focusing are of course not taken into account in a 1HD model. However, one advantage of this model is that it can apply

grids of variable resolutions, allowing for finer grids in the shallowest waters. In the simulations we have designed the spatial grid to keep the Courant number (i.e. the ratio of the spatial grid increment to the temporal grid increment; Courant et al. 1967) constant. For a defined temporal resolution the spatial resolution is coarser in deeper water, enabling fewer grid cells and less CPU time spent. This is an advantage for tsunami modelling since higher resolution is needed in shallower areas to resolve the waves (waves become shorter) and since the presence of numerical dispersion is minimized due to a constant Courant number. Grid refinement tests were performed to ensure convergence for each run. For the 1HD simulations the Courant number was set to 0.5 with a temporal increment of 2.5 s, giving a spatial resolution from 34 m close to the shoreline up to 500 m in the deepest part. In the 2HD simulations around smaller islands the uniform spatial resolution was 500 m.

Although the models do not include the inundation on dry land, the surface elevation on the boundary close to the shoreline (at 0.5 m water depth) with a no-flux condition yields a good approximation. The results from the depth averaged models are validated by a subset of corresponding simulations performed with 1HD and 2HD nonlinear inundation models including shock waves and wave breaking (Løvholt et al. 2011; NGI 2009c).

The results show that the 1HD tsunami model applied in the present study estimates the shoreline water level mainly with a deviation of less than 20-30% from the nonlinear model. However, larger deviation may occur for very long and gentle slopes due to omission of wave breaking. For a M_W 8 earthquake scenario (Lesser Antilles scenario as explained in Section 5.1) east of Guadeloupe, the regional approach based on the amplification factors gave a maximum shoreline water level of 2.6 m at Bridgetown, while a corresponding study with a 2HD model gave a run-up height of 2.9 m (NGI 2009a; Løvholt et al. 2011). Naturally, we expect that the regional methodology do not capture local variations. However, for the purpose of a regional study, the approach gives reasonable results on the overall scale.

5 Tsunamigenic source scenarios

The scenario selection is principally based on a comprehensive analysis of the updated database on both seismic and non-seismic Caribbean tsunami events (above), a literature survey on non-seismic

tsunamigenic sources in the region (NGI 2009c), the study of the large scale tectonics of the region by NORSAR (NGI 2009b), geological and topographical evaluations, information from R. Robertson, SRC (pers. comm., 2007-2008), and the Volcanic Hazard Atlas of the Lesser Antilles (Lindsay et al. 2005). It should be noted that all areas have not been similarly well surveyed, nor have the survey data been available in order to evaluate the potential for tsunamigenic sources to the same extent all over the region. This is especially relevant for potential submarine landslides along the margins of the Caribbean Sea (Teeuw et al. 2009).

In addition to sensible choices based on all the sources of information listed above, the tsunami scenarios for this study should also represent various types of sources, provide a regional distribution to exemplify a regional exposure assessment, provide relevant examples for all partners in the project, avoid reproduction of previous studies, and be relevant as input for the Bridgetown tsunami Disaster Mitigation Demonstration Project (NGI 2009a). The tsunami surface elevations shortly after the initiation of the five selected Caribbean scenarios are shown in Figure 5, and an example of a trans-oceanic tsunami scenario is presented in Section 5.3.

5.1 Seismic scenarios

The Northern coastlines of Hispaniola and Puerto Rico were hit by 5 to 6 m tsunamis in 1918 and 1946 and we chose the subduction earthquake located on the strait between the two islands as a source scenario (hereafter called the Hispaniola scenario)[1]. The northeast Lesser Antilles were hit in 1843 by the largest reported historical earthquake of the Lesser Antilles subduction arc (hereafter called the Lesser Antilles scenario). It produced seismic intensity IX on a segment about 100 km long between Antigua and Guadeloupe and generated a small tsunami.

[1] It should be noted that López-Venegas et al. (2008) identified a submarine landslide off the northwestern coast of Puerto Rico, and postulate that this landslide, which was likely triggered by the 1918 earthquake, was the primary cause of the October 11, 1918, tsunami.

An M_W 8 scenario represents a credible worst case earthquake scenario based on the 500 year history of earthquakes and tsunamis in the Caribbean region (NGI 2009b, 2009c). Parsons and Geist (2009) state that the completeness threshold varies with time, and is likely about M_W 7 before the 20th century. Parsons and Geist (2009) further estimate a total tectonic moment for a 505-year period corresponding to M_W 9.18 and report an expressed seismic moment sum from the earthquake catalogue corresponding to M_W 8.85. This implies that the coupling coefficient (i.e. the ratio of expressed seismic to expected tectonic moment release) around the Caribbean plate is low, or that there is a large temporal seismic gap waiting to be expressed. Both the Lesser Antilles and the Hispaniola scenarios are built up by three fault segments, with a tapering of the co-seismic slip at the end-segments. The scenarios are close to identical except for location and orientation. The fault models are about 180 km long with slips of 6 m for the central segment and 3 m (mid value) for the end segments (seismic source geometries are listed in Table 2). The rigidity is set to 30 MPa (Bilek and Lay 1999). Length, width, and slip are parameterised based on the empirical expressions by Wells and Coppersmith (1994).

Lesser Antilles scenario

The source model in this case is based on the January 30, 1982, M_W 6 thrust event and its Harvard CMT solution. The fault plane chosen for the tsunami modelling has a strike of 340° and a dip of 80°. Its conjugate fault plane (strike of 166° and dip of 11°) might be more compatible with the regional tectonics, but it would have generated a smaller seabed elevation (Løvholt et al. in revision). However, the purpose of this simulation is to estimate the credible worst scenario. This fault model scenario is also steeper than the average dip angle of the Wadati-Benioff plane and may therefore generate shorter waves favouring stronger amplification due to shoaling. The maximum tsunami surface elevation calculated in each computational cell during the total computational time is shown in Figure 6. The values in shallow/near shore areas may be underestimated; the corresponding maximum shore line water levels landward from the control points are shown in Figure 7.

The estimated maximum surface elevations and maximum shoreline water levels show that the Lesser Antilles scenario affects mostly the eastern part of the Lesser Antilles arc. The highest waves are found in an area directed east-west. The sea surface elevation around the generation area is 1-4 m, while the

islands south and north of the most affected ones have sea surface elevations off the shore above 0.5 m. There is some effect of the tsunami (~0.5 m) found also in the southern part of Puerto Rico and along the north-western coast of Venezuela. The rest of the Caribbean Sea is only slightly affected. The area west of the Lesser Antilles arc is protected by the islands closest to the source area. This scenario is applied further in a local and more detailed tsunami vulnerability and risk analysis for Bridgetown, Barbados (NGI 2009a).

Hispaniola Antilles scenario

The source model here is based on the June 24, 1984, M_W 6.7 thrust event and its Harvard CMT solution. The fault plane chosen for the tsunami modelling has a strike of 100° and a dip of 80°. Again, the conjugate fault plane which is much shallower dipping is more compatible with the regional tectonics, but the worst scenario was preferred for the tsunami modelling. The maximum tsunami surface elevation calculated in each computational cell during the total computational time is shown in Figure 6. The tsunami from the Hispaniola scenario is directed more north-south, and especially impacts the north-eastern part of Hispaniola and parts of Puerto Rico. The values in shallow/near shore areas may be underestimated, but the corresponding maximum shore line water levels landward from the control points are shown in Figure 7. The offshore surface elevations are up to 10 m locally. The Hispaniola and Puerto Rico islands serve as a shield protecting the rest of the Caribbean Sea. An exception occurs where the waves entering between Hispaniola and Puerto Rico hit the coast of the northern part of Venezuela and Colombia. However, due to diffraction and radial spread the offshore surface elevation there is below 0.5 m.

5.2 Non seismic scenarios

Two subaerial/submarine volcano debris flow scenarios and one submarine landslide scenario are selected to demonstrate non-seismic sources. The model parameters for all three scenarios are found in Table 34 with the dimensions of the simplified rounded box landslide, the submarine run-out distance, as well as the impact velocity, V_{max}.

Montserrat scenario

The eruptive Soufrière Hills volcano on Montserrat has generated several small tsunamis in the recent past (1997, 1999, 2003, and 2006). We simulate a $1.7 \cdot 10^8$ m^3 landslide scenario mimicking a flank collapse in the English's Crater on the eastern side of the cone, and this volume corresponds approximately to the 4000 BP event. Le Friant et al. (2004) argue that the corresponding deposits were formed by one event. The simulated scenario can therefore be considered a subaerial/submarine worst case for the Soufrière Hills volcano. For comparison, the 1997 event had a volume of $2.5 \cdot 10^7$ m^3, while the 2003 event had a larger volume ($2 \cdot 10^8$ m^3), but reached the sea as a series of smaller landslides with limited velocities.

The Montserrat scenario is clearly the most local of the five scenarios evaluated in this study (Figure 8 and Figure 9). The maximum offshore surface elevation is 2.5 m, but it has minor effects on the islands south of Guadeloupe and west of the Lesser Antilles arc. In contrast to the earthquake scenarios where the maximum waves have a clear directional propagation, the landslide scenarios act more or less as point sources with no pronounced directivity. The results agree reasonably well with simulations by Heinrich et al. (1998; 1999), when taking their smaller volume of $40 \cdot 10^6$ m^3 (as for the 26 December 1997 event) and larger impact velocity of 40 m/s into account.

Saint Lucia scenario

According to Lindsay et al. (2005), a possible scenario for a magmatic eruption is a dome-forming eruption from within the Qualibou Caldera on Saint Lucia (this is not the least-likely worst case large explosive magmatic eruption scenario). Such an eruption would be similar to the ongoing eruption of the Soufrière Hills volcano in Montserrat and may generate, among others, dome-collapse pyroclastic flows. Lack of age data makes it impossible to develop an eruption frequency. However, the major activity seems to have been concentrated 35 000 – 20 000 years BP. It should be kept in mind that pyroclastic deposits are easily eroded, and it is possible that more eruptions have occurred over the last 20 000 years and that their products have not been preserved.

We consider a subaerial/submarine landslide from the Soufrière volcanic centre cone in Saint Lucia. Due to the combination of large volume, higher velocity, and longer run-out, the Saint Lucia scenario has a significantly greater impact in large areas than the Montserrat scenario (Figure 8 and Figure 9). Locally the offshore surface elevations are above 10 m, and the surface elevation on the west side of the islands from the Virgin Islands down to Dominica is between 0.5 and 1 m. From Dominica down to Grenada, the elevation is between 3 and 10 m. Waves leak between Saint Lucia and Saint Vincent and the Grenadines, forming a south-easterly directed pattern south of Barbados. The surface elevation outside Bridgetown, Barbados is about 0.6 m.

Kick'em Jenny scenario

Kick'em Jenny 8 km north of Grenada is the most active volcanic centre in the Lesser Antilles arc. Based on the bathymetry and the information cited above, the tsunami generated by a 0.6 km^3 submarine landslide running westward on the flanks of the submerged volcano cone is simulated. The simulated waves are slightly lower than the St. Lucia scenario (Figure 8 and Figure 9). The main part of the waves is kept on the western side of the Lesser Antilles arc. Some parts of the waves have a direction towards Puerto Rico and Hispaniola, leading to offshore surface elevations there between 0.5 and 1 m.

5.3 Extreme transoceanic scenario

Possible transoceanic tsunamis threatening the Caribbean Islands may be generated by strong earthquakes from distant seismic zones, or alternatively, by large submarine or subaerial landslides. One example of a strong earthquake is the 1755 Lisbon earthquake (Baptista et al. 1998; 2003; Gutscher et al. 2006; Horsburgh et al. 2008, Roger et al. 2010, Barkan et al. 2009), which generated a tsunami that killed more than 30 000 people in Portugal. The tsunami probably also maintained large amplitudes across the Atlantic Ocean. Potential non-seismic transoceanic sources may for instance include submarine landslides off the continental margin of western Africa, or subaerial and submarine landslides originating from the Canary and Cape Verde Islands (less likely from the Azores Islands). One of the most extreme scenarios would be a collapse of the La Cumbre Vieja volcano on the island of La Palma, releasing a volume of 375 km^3 simultaneously. The threat of such a scenario has been addressed by Ward and Day

(2001), Mader (2001), Pararas-Carayannis (2002), Gisler et al. (2006a), and Løvholt et al. (2008). In Løvholt et al. (2008), near shore surface elevations of 5-15 m are found from Northern Brazil north to New York City, in addition to the enormous local waves generated along the coastlines of the Canary Islands and more nearby locations. Even larger waves are found by Ward and Day (2001), whereas Mader (2001) predicts clearly smaller waves.

5.4 Scenario return periods

A scenario is by definition not associated with an occurrence probability, since the only requirement is that it should only be within the realm of the possible. Even so, to be useful in a hazard and risk context, the applied scenarios should still be presented with some indication of likelihood. To this end, an attempt to roughly estimate possible return periods is presented below.

Seismic sources

Løvholt et al. (2006) found that for South America, Japan, and Sunda Arc combined, 34% of the shallow earthquakes with M≥7 were reported to have generated a tsunami, with 71% for M≥7.5 and 84% for M≥8.0. For reference, the probability that a shallow M≥7 earthquake occurs in the Puerto Rico region is 0.61 per decade (Panagiotopoulos 1995).

The historical seismic database in the Caribbean is too short to estimate the earthquake potentials with confidence and the geologic framework is also quite complicated, but the largest credible earthquake for the entire region is estimated to be around M8 and with a return period of around 500 years, which corresponds to the duration of the historical records. A more detailed discussion on the return period of the tsunamigenic earthquakes is given by Parsons and Geist (2009), who complemented the earthquake and tsunami records with computations of the seismic moment balance, finding slip rates typically ranging from 5-15 m over 500 years in the Lesser Antilles, whereas slip rates of 1-3 m over 500 years were found from the historical records. By assuming a locked fault and a slip of 6 m, the seismic moment balance corresponds to lower bound return periods of about 200-500 years for the earthquake scenarios. Grilli et al. (2010) state that a M_w9.1 source corresponds to a 600 year or so return period,

while a M_w8.7 source corresponds to a 200 year or so return period. Zahibo et al. (2008) suggest M8 earthquake return periods of about 200 years. It should be noted that the individual tsunami scenario return periods are generally longer than the lower bound earthquake return periods, partly because an individual earthquake scenario has a longer return period than the return period for the corresponding earthquake magnitudes in question within the study region, and partly because only some of the earthquakes will be tsunamigenic.

Non-seismic sources

Ten Brink et al. (2006a) calculated the return periods of submarine landslide in the Puerto Rico trench by considering the number of large failures. For the Loiza amphitheatre the average recurrence rate is about 250-825 ka and it is about 130-470 ka for the Arecibo amphitheatre. The combined landslide tsunami recurrence rate for the north coast of Puerto Rico from the entire carbonate platform is about 70-250 ka. In comparison, Kick'em Jenny has erupted at about 5 year intervals since 1939. Ten Brink et al. (2006b) established a power-law volume frequency distribution for submarine slope failures north of Puerto Rico.

Deplus et al. (2001) state that the age of the large-scale debris flows mapped offshore of the Lesser Antilles Arc is younger than 100-200 ka. Boudon et al. (2007) identified 15 flank collapses within the last 12 ka in the Lesser Antilles Arc (there may have been several collapses from the same volcano, and not all flows enter the sea even though the Caribbean Islands are small). The Lesser Antilles include 21 live volcanoes that could erupt in the future (Lindsay et al. 2005). From this information, a rough estimate gives a collapse return period of 20 000 years for each volcano (~20 sources causing ~10 collapses during ~10 000 years). Boudon et al. (2007) further state that in the northern part of the arc, flank collapses are smaller (~1 km^3), repetitive, and occur in all directions. In contrast, larger (up to tens of km^3) and infrequent sector collapses all directed to the west are typical in the southern part.

A rough estimate based on the age determination data from deposits of Holocene tsunami events in the wider Caribbean by Scheffers and Kelletat (2006) gives a return period of 1000-3000 years. However, their data may originate from the same tsunami event being detected in several places, i.e. high energy

tsunami sources have return periods longer than 3000 years. On the other hand, small deposits suffer erosion and may disappear. Scheffers and Kelletat (2006) say further that "risk analyses […] based solely upon historical sources underestimate the real tsunami risk by a factor of five to ten and the so far neglected coasts facing the open Atlantic Ocean are particularly endangered."

In summary, the individual return period of the smaller non-seismic events in the northern part of the arc can be estimated to be more than 1000 years, while the individual return period of larger events in the southern part of the arc is more on the order of 10 000 years. It should also be mentioned that Zahibo and Pelinovsky (2001) estimate the return period for all kinds of tsunamis (seismic and non-seismic tsunamis) in the Lesser Antilles exceeding 2-3 m to be 100 years.

Extreme transoceanic sources

In the latest 1 Ma or so, the Canary Islands have produced one large landslide approximately every 100 ka, with typical volumes of 50-200 km^3 (Masson et al. 2006). However, these landslides are believed to develop retrogressively (Wynn and Masson 2003), and thus being less effective in generating a tsunami than a single volume. As pointed out by Wynn and Masson (2003), the separation time between each landslide volume is expected to be so large that a visible contrast in the turbidite deposit may be identified for each retrogressive element comprising the total volume. The effective tsunamigenic volume is therefore likely to be significantly smaller than the total volume.

A simultaneous release of a landslide may however not be completely ruled out, both because the retrogressive effects are not quantified, and also because a future landslide does not necessarily follow the nature of previous landslides. For a simultaneously and extreme released volume of 375 km^3 we expect that the annual probability is clearly smaller than the 10^{-5} obtained from the recurrence rate of all the past landslide events within the Canaries, taking into account that a gradual release of the slide is more likely. An expert judgment may crudely suggest an annual probability of at least one order of magnitude less, i.e. roughly < 10^{-6}. Still, it may obviously be disputed whether it is at all possible to quantify this return period. It is also noted that the risk of the extreme event may exceed the more likely ones as the consequence may increase faster than the probability decays. This extreme event should

therefore be studied. However, in the future it is important to include a study of a smaller and more realistic volume and investigate its far-field impact. The low probability combined with longer arrival times and thereby longer warning times and reduced risk for trans-oceanic tsunamis, substantiates why this scenario is not pursued further in this study.

5.5 Tsunami simulations and results

Seismic and non seismic Caribbean scenarios

The maximum tsunami surface elevation calculated in each computational cell is shown in Figure 6 and Figure 8 for all five scenarios. The maximum surface elevation should not, however, be used to determine the impact on land (i.e. how high the waves are near the shore or during inundation) since the near shore amplification is not captured in the simulations. The waves typically amplify several times on their way towards the shoreline, and these effects are taken into account in the estimations of the maximum shoreline water levels in Figure 7 and Figure 9. In the simulations, the uniform spatial resolution was 1' (about 1.85 km).

The highest waves for the earthquake scenarios are of course found closest to the sources, with values up to about 20 m (Hispaniola/Puerto Rico and east part of Guadeloupe and the surrounding islands). The waves for the landslide scenarios along the islands in the eastern part of the Caribbean Sea are mainly in the range of 1-5 meters. Close to the landslide areas, the maximum shoreline water levels can be several times higher. The predicted arrival times for the two furthest north and south scenarios (i.e. Hispaniola and Kick'em Jenny) are depicted in Figure 10. The tsunami arrival time is generally short for the Caribbean Islands; typically one should prepare for less than one hour.

Extreme transoceanic scenario

For this study, we combined results of the numerical simulations by Gisler et al. (2006a) for the wave propagation in the central Atlantic Ocean and Løvholt et al. (2008) for a local simulation of the tsunami propagation near the Lesser Antilles. The overall trends rather than detailed results are investigated.

Gisler et al. (2006a) used the numerical model SAGE (Gittings et al. 2008) to simulate the simultaneous landslide and water wave motion. The landslide motion was close to critical with a maximum landslide speed up to approximately 150 m/s, effectively generating a large tsunami. The far-field propagation was simulated using the Globouss model. For the transatlantic propagation in Løvholt et al. (2008), a grid resolution of 2' was used. In our local simulations near the Lesser Antilles, the results from the Atlantic propagation are extracted and used as initial conditions in a smaller domain covering the Lesser Antilles. In our computations, different grid resolutions of 2', 1', and 0.5' are used (the two latter are interpolated from the 2' grid using bi-linear interpolation). Along the Northern, Western, and Southern boundaries, an absorbing layer of width 0.4° is used, whereas the Eastern boundary is reflective.

Snapshots of the simulated extreme wave as it approaches and impacts the Caribbean Islands are shown in

Figure *11*. A sequence of large incident waves is observed. The increased wave heights, especially towards Trinidad and Tobago, result as a combination of refraction and source directivity. The maximum run-up heights are expected to clearly exceed the maximum offshore surface elevations of 5-10 m typically found in the locations displayed in

Figure *11* (at depths of 500 m or more) as a result of amplification due to shoaling. Effects of edge waves, interference of reflecting waves, etc., may also enhance the maximum water levels.

Figure 11 further reveals that the wavelengths in question are generally longer than the typical extensions of the islands, which together with the steep shelves prevents significant amplification due to shoaling. In addition, it is expected that possible wave breaking and friction will to some extent counteract the amplification.

Figure *11* also shows how the Lesser Antilles provide a screening for the westerly located islands and coastlines.

The solution converged for the first few wave cycles for most of the locations in

Figure 11 (NGI 2009c). An exception was the Barbados west location (site C). In time series from other locations not displayed here, there is generally a tendency that the time series affected by island reflection etc., tend to give results that deviate more. However, the eastward time series are less

influenced by such effects, and better accuracy is therefore found in these locations (site A, B, D, E, and F).

6 Regional exposure assessment

One of the main goals for a study of this kind is clearly to estimate the number of people exposed to the tsunamis triggered by landslides and earthquakes in the region, and to this end we have employed a GIS analysis. The maximum water level raster along the shoreline has been interpolated from the shoreline water level points using the Inverse Distance Weighted (IDW) method, and the inundated area is obtained by subtracting a digital elevation model with 3 arc seconds resolution from the shoreline maximum water level raster (NGI 2009c). Hence, the inundated area first covered all the topography below the maximum shoreline water level. However, it turned out that for some gentle and low-lying near shore locations, the inundation distance could be unreasonably long. A simple formula was therefore used to limit the maximum inundation distance:

$$I_{\max} = \sqrt{g\eta} \cdot T / 4$$

where η is the maximum shoreline waver level, g the acceleration of gravity, and T the wave period set to 600 s (the wave period for the combination of slide- and earthquake-generated waves varies from 400 s to 1000 s with a mean value of about 600 s). The formula assumes that the wave travels inland with a propagation speed of $(g\eta)^{1/2}$ for a quarter of a predefined wave period (i.e. during the time the tsunami is still rising at the shore line), and therefore gives a rough upper bound of the inundation length. The expression is obviously inaccurate (the wave can travel faster inland than $(g\eta)^{½}$ from the beginning of the inundation, the flow depth decreases and causes lower velocities further inland, the wave can travel inwards for a longer time than *T/4*, obstructions influence the travel distance, etc.), but we still believe that it is a good first order approximation of inundation distance for a regional study.

The Shuttle Radar Topography Mission (SRTM) elevation data used here is the most complete high-resolution digital topographic database available to us (Rabus et al. 2003). The population dataset is taken from the Global Rural-Urban Mapping Project (GRUMP) which consists of estimates of human population for the years 2007 (CIESIN 2007) and has a spatial resolution of 30 arc seconds. The exposed population is defined as the number of people in the inundated areas. The exposed population per km shoreline is created by manually defining line segments along the coast with approximately similar population density per unit area. The statistics from these areas are then projected into the shoreline for the same area.

During the last century, a relative sea level rise of about 20 cm has been observed in the Caribbean and the rate is increasing. Relative sea level was estimated to rise on average 2.8 - 5.0 mm/year during the 1990's. Regional projections state a rise in sea level of 10 - 50 cm by 2025 as realistic (Maul 1993; Parry et al. 2007). Moreover, the global sea level rise within year 2100 is estimated to be in the range from 20 to 50 cm (Bindoff et al. 2007). Inside the Caribbean region the high tide is about 50 to 90 cm above mean lower low water (NOAA 2008). The topography is measured relative to mean sea level (MSL). A high tide may roughly be set to 25-45 cm above MSL. A combined effect of sea level rise and high tide is taken into account in our investigations by adding 0.7 m to the estimated maximum shoreline water levels. The probability of two independent extreme events, namely a design tsunami and an extreme high tide, happening at the same time is so low that it contributes very little to the total hazard.

Figure 2 and Figure 12 show the number of people exposed to landslide or earthquake induced tsunamis in the Caribbean region. The results for the two groups of tsunamigenic sources are kept separate owing to different estimated probabilities. The different colour scales in the figures should be noted. The total number of exposed people for each country is presented in Figure 13 for the seismic sources and in Figure 14 for the landslides sources. The exposure is presented both as the total number of exposed people and as a percentage of the total number of inhabitants in each country. The tsunami exposure with and without the effect of possible sea level rise and high tide is also compared. The strongest effect of higher sea level is found for Puerto Rico (total exposure), Antigua and Barbuda and Anguilla (relative exposure) both for the earthquake and landslide scenarios, and for Venezuela (total exposure) and Saint Lucia (relative exposure) for the landslide scenarios. The high exposure along the coasts of Puerto Rico and the southern coast of the Dominican Republic is due to the very gentle, low-lying terrain and dense

population. For the earthquake scenarios, Puerto Rico (90 000 exposed people), Venezuela (50 000), the Dominican Republic (35 000), and Guadeloupe (30 000) have the highest exposure in terms of total number of people. The highest exposure relative to the population is found in Antigua (7.5%) and in Guadeloupe (6.5%).

The highest number of exposed people for the landslide scenarios is found for Venezuela (50 000 exposed people), while there are several countries with approximately 10 000 people exposed (Saint Lucia, Puerto Rico, Haiti, Dominican Republic, and Colombia). Antigua (5%) and Saint Lucia (4.5%) have the highest exposure relative to the population. The fact that a landslide acts as a point source with possible higher damping rates than for earthquake sources can also be seen by comparing Figure 2 and Figure 12.

The exposure for Venezuela is high (in terms of total number of exposed people) for both types of scenarios. This is due to both the effect of low topography and of course high coastal population density. In Figure 15 and Figure 16 the distribution of the exposure is shown as an example for Antigua which is the most exposed island relative to its population according to our study. The two maps are very similar and therefore the same mitigation measures should be put in place for the two sources of tsunamis. Predicted tsunami arrival times vary between about 30 min (for the Lesser Antilles scenario) to 2 hrs 20 min (for the Hispaniola and Kick'em Jenny scenarios, Figure 10).

It should be noted that the results may be biased owing to the limited number of scenarios assessed, implying higher surface elevations and number of exposed people in the vicinity of the presented tsunami source areas. This is especially relevant for the near shore and non-seismic tsunami scenarios. Further, the resolution of the bathymetry, elevation, and population data is too coarse for the hazard and exposure maps to be applied at a local scale.

7 Concluding remarks

A tsunami exposure assessment for the Caribbean region is performed. Compared to previous studies, a first step forward is that both seismic and non-seismic tsunamigenic sources are studied together, enabling a more complete hazard and exposure comparison. The probability, location, and size of the

largest credible earthquake and gravity mass flow tsunami sources are based on historical earthquake and tsunami occurrence, large scale tectonics, and geology. Both submarine and initially subaerial tsunamigenic debris flows and landslides are included. The seabed displacements related to earthquakes are determined by analytical calculations, while the seabed displacements and mass flow dynamics related to mass flows are determined by a combination of analytical calculations and numerical simulations. The seabed displacements are used as input to the numerical tsunami simulations. Both linear hydrostatic and non-linear dispersive (Boussinesq) models are applied to describe the tsunami propagation. Dispersive effects turn out to be particularly important for the trans-oceanic tsunamis.

A second step forward compared to earlier tsunami studies for the Caribbean is the use of a recently developed procedure to transfer the offshore tsunami surface elevation to the shoreline water levels, determining the amplification factors from the parameters describing the incoming wave and bathymetric slope. Possible overestimation is due to lack of friction and breaking in the method of amplification factors. Finally, the total number of people exposed to the tsunamis triggered by landslides and earthquakes in the region is estimated, applying the maximum shoreline water level, a high-resolution digital topographic database, and a population dataset in a GIS analysis.

Large scale tectonics and compilation of the historical data for hazardous tsunami events in the region indicate that the return period for the selected M_W 8 earthquake tsunami scenarios is to the order of 500 years. The return period for landslide triggered tsunami scenarios is even more difficult to estimate, but the individual return period of the smaller non-seismic events in the northern part of the arc can be estimated to more than 1000 years, while the individual return period of larger events in the southern part of the arc is more along the order of 10 000 years. It should be noted that the return periods for the future tsunamis are not to be interpreted as precise estimates. For the seismic scenarios, the “memory free” (i.e. the probability of a future event is independent of the occurrence of recent events) assumption should be alluded. For the non-seismic scenarios, a more precise quantification of the probabilities could probably be achieved by in-depth individual studies of the potential landslide and debris flow source areas.

A maximum shoreline water level up to about 20 meters is found closest to the sources (Hispaniola/Puerto Rico and the eastern section of Guadeloupe and the surrounding islands) for the seismically induced tsunami scenarios. The maximum shoreline water level for the landslide tsunami scenarios along the islands in the eastern part of the Caribbean Sea is mainly in the range of 1-5 meters. Locally, the shoreline water level can be several times higher close to the landslide areas. A volcano flank collapse from the Soufrière Volcano at Saint Lucia is found to give maximum shoreline water levels of 3-10 m in the coastal areas from Dominica down to Grenada.

Using predicted tsunami maximum shoreline water levels together with available population data, it is found that Puerto Rico is the most exposed island, with as many as 90 000 people located in the likely tsunami inundation zones for the 500 years earthquake events that have been selected. Other highly exposed countries are Venezuela with 50 000, the Dominican Republic with 35 000, and Guadeloupe with 30 000 people. Measuring exposure relative to the population, Antigua is highest with 7.5%, followed by Guadeloupe with 6.5%. Exposure for tsunamis triggered by the selected landslide sources shows the highest figure for Venezuela (50 000 people), while there are several countries with approximately 10 000 people exposed (Saint Lucia, Puerto Rico, Haiti, Dominican Republic, and Colombia). The total risk is probably higher for the earthquake induced tsunamis than for the landslide induced tsunamis, owing to a higher number of exposed people and a shorter return period. The tsunami arrival time is generally short for the Caribbean Islands, typically one should prepare for less than one hour. This will certainly influence on the design and effectiveness of a tsunami early warning system and the possibility of evacuating the residents.

The presented regional hazard maps and population exposure are based on approximate and simplified methods as well as coarse resolution bathymetry, elevation, and population data to cover large geographical areas. Such hazard maps should therefore not be interpreted nor applied locally, but rather as a tool to produce reasonable regional estimates for risk comparison and management. The scenarios cover only the presumably most important ones. Hence, the results may be biased owing to the limited number of scenarios assessed. A higher number of sources would reveal a more complete picture of the regional tsunami risk. This would also illuminate the risk related to more frequent, but lower energy scenario sources. Finally, the maximum water levels, the inundated areas, and the resulting exposure of

people should be further investigated, preferably with higher data resolution, in certain areas of complex terrain.

Acknowledgements

L. Brewster, L. Inniss, F.Hinds, and R. Roach (CZMU Barbados), R. Mahon, L. Nurse, N. Gour, J. Blackwood, and R. Goodridge (UWI/CERMES Cave Hill Barbados), R. Robertson and L. Lynch (SRC Trinidad), R. Ahmad (UWI Mona, Jamaica), J. Collymore, E. Riley, and A. Brome (CDERA Barbados), J. Thomas (DEM Barbados), as well as disaster coordinators throughout the Caribbean region are all thanked for helpful support to render possible and facilitate the project, including information and data sharing, arranging workshops and seminars, and capacity building. R. Goodridge is thanked for her assistance with the linguistics of the manuscript. The Norwegian Ministry of Foreign Affairs is greatly acknowledged for the financial support to execute the 2006-2008 UWI/NGI capacity building program on natural disasters mitigation in the Caribbean. The Norwegian Geotechnical Institute (NGI), the International Centre for Geohazards (ICG), NORSAR, the Institut de Physique du Globe de Paris (IPGP), and the Research Council of Norway are thanked for supporting the conversion of the project reports into this journal paper . Finally, the two anonymous referees are thanked for valuable comments to the manuscript. This is contribution no. 372 of the International Centre for Geohazards.

References

Baptista M A, Heitor S, Miranda J M, Miranda P, Mendes L (1998) The 1755 Lisbon Tsunami; Evaluation of the tsunami parameters. J Geodynamics 25 (2):143-157

Baptista M A, Miranda J M, Chierici F, Zitellini N (2003) New study of the 1755 earthquake source based on multi-channel seismic survey data and tsunami modeling. Natural Hazards and Earth System Sciences 3:333–340

Barkan R, ten Brink U S (2010) Tsunami Simulations of the 1867 Virgin Island Earthquake: Constraints on Epicenter Location and fault Parameters. Bulletin of the Seismological Society of America 100 (3):995-1009.

Barkan R, ten Brink U S, Lin J (2009) Far field tsunami simulations of te 1755 Lisbon earthquake. Implications for tsunami hazard to the U.S. East Coast and the Caribbean. Marine Geology 264:109-122

Bengoubou-Valérius M, Bazin S, Bertil D, Beauducel F, Bosson A (2008) CDSA: A new seismological data center for French Lesser Antilles. Seismological Research Letters 79:90-102

Bernard P and Lambert J (1988) Subduction and seismic hazard in the Northern Lesser Antilles: Revision of the historical seismicity. Bulletin of the Seismological Society of America 78:1965-1983

Bilek S L, Lay T (1999) Rigidity variations with depth along interplate megathrust faults in subduction zones. Nature 400:443-446

Bindoff N L, Willebrand J, Artale V, Cazenave A, Gregory J, Gulev S, Hanawa K, Le Quere C, Levitus S, Nojiri Y, Shum C K, Talley L D, Unnikrishnan A (2007) Observations: Oceanic Climate Change and Sea Level. In Solomon S, Qin D, Manning M, Chen Z, Marquis M, Averyt K B, Tignor M, and Miller H

L (eds). Climate Change 2007: The Physical Science Basis. Contribution of Working Group I to the fourth assessment report of the intergovernmental panel on climate change. Cambridge University Press, Cambridge

Boudon G, Le Friant A, Komorowski J C, Deplus C, Semet M P (2007) Volcano flank instability in the Lesser Antilles Arc: Diversity of scale processes and temporal recurrence. Journal of Geophysical Research 112 doi: 101029/2006JB004674

BRGM (2009) Data extracted from Tsunamis. BRGM 2009 www.tsunamis.fr

Brown G M, Holland J G, Sigurdsson H, Tomblin J F, Arculus R J (1977) Geochemistry of the Lesser Antilles volcanic island arc. Geochimica et Cosmochimica Acta 41:785-801

Calais E, Freed A, Mattioli G, Amelung F, Jónsson S, Jansma P, Hong S-H, Dixon T, Prépetit C, Momplaisir R (2010) Transpressional rupture of an unmapped fault during the 2010 Haiti earthquake. Nature Geoscience 3, 794–799, doi:10.1038/ngeo992
http://www.nature.com/ngeo/focus/haiti/index.html

Calais E, Perrot J, Mercier de Lepinay B (1998) Strike-slip tectonics and seismicity along the northern Caribbean plate boundary from Cuba to Hispaniola. In Dolan J F, Mann P (eds). Active Tectonics of the Northern Caribbean Plate Boundary Zone, GSA Special Paper 326:125-141

Carlson R L, Raskin G S (1983) Density of the ocean crust. Nature 311:555-558

Center for International Earth Science Information Network (CIESIN) (2007) Columbia University; International Food Policy Research Institute (IPFRI) the World Bank; and Centro Internacional de Agricultura Tropical (CIAT) Global Rural-Urban Mapping Project (GRUMP): Gridded Population of the World available at: http://beta.sedac.ciesin.columbia.edu/gpw Courant R, Friedrichs K, Lewy, H (1967) On the Partial Difference Equations of Mathematical Physics. IBM J. 11, 215-234

De Blasio F V, Elverhøi A, Engvik L, Issler D, Gauer P, Harbitz C B (2006) Understanding the high mobility of subaqueous debris flows. Norwegian Journal of Geology 86:275-284

de Buisonje P H, Zonneveld J I S (1976) Caracasbaai: A submarine slide of a high coastal fragment in Curaçao. Nieuwe West-Indische gids 5:55-88

DeMets C, Jansma P E, Mattioli G S, Dixon T H, Farina F, Bilham R, Calais E, Mann P (2000) GPS geodetic constraints on Caribbean–North America plate motion. Geophysical Research Letters 27:437-440

Deplus C, Le Friant A, Boudon G, Komorowski J C, Villemant B, Harford C, Segoufin J, Cheminee J L (2001) Submarine evidence for large-scale debris avalanches in the Lesser Antilles Arc. Earth and Planetary Science Letters 192(2):145-157

Dorel J (1981) Seismicity and seismic gap in the Lesser Antilles arc and earthquake hazard in Guadeloupe. Geophysical Journal of the Royal Astronomical Society 67:679–695

Engdahl E R, Villaseñor A (2002) Global Seismicity: 1900-1999. IASPEI International Handbook of Earthquake and Engineering Seismology 81:665-690

Engdahl E R, Villaseñor A, DeShon H R, Thurber C H (2007) Teleseismic Relocation and Assessment of Seismicity (1918–2005) in the Region of the 2004 Mw 9.0 Sumatra-Andaman and 2005 Mw 8.6 Nias Island Great Earthquakes. Bulletin of the Seismological Society of America 97(1A):43-61

Feuillet N, Manighetti I,Tapponnier P (2002) Arc parallel extension and localization of volcanic complexes in Guadeloupe Lesser Antilles. Journal of Geophysical Research 107 (B12) 2331

GEBCO (2008) Information and downloadable data at http://www.bodc.ac.uk/products/bodc_products/gebco/ (Accessed December 2008)

Girardin N, Feuillard M, Viodé J P (1991) Réseau régional sismique de l'arc des Petites Antilles: Sismicité superficielle (1981-1988). Bulletin de la Société Géologique de France 162(6):1003-1015

Girardin N, Gaulon R (1982) Microseismicity and stresses in the Lesser Antilles dipping seismic zone. Earth and Planetary Science Letters 62:340-348

Gisler G, Weaver R, Gittings M (2006a) SAGE calculations of the tsunami threat from La Palma. Science of Tsunami Hazards 24:288-301

Gisler G, Weaver R, Mader C, Gittings M (2006b) Two-Dimensional Simulations of Explosive Eruptions of Kick'em Jenny and other Submarine Volcanoes. Science of Tsunami Hazards 25(1):34-41

Gittings M, Weaver R, Clover M, Betlach T, Byrne N, Coker R, Dendy E, Hueckstaedt R, New K, Oakes W R, Ranta D, Stefan R (2008) The RAGE radiation-hydrodynamic code. Computational Science & Discovery 1, 015005, 63 pp doi:10.1088/1749-4699/1/1/015005 http://iopscience.iop.org/1749-4699/1/1/015005/pdf/1749-4699_1_1_015005.pdf

Grilli S T, Dubosq S, Pophet N, Pérignon Y, Kirby, J T, Shi F (2010) Numerical simulation and first-order analysis of large co-sesimic tsunamis generated in the Puerto Rico trench: near-field impact on the North shore of Puerto Rico and far-field impact on the US East Coast. Natural Hazards and Earth System Sciences 10:2109-2125

Gutscher M-A, Baptista M A, Miranda, J M (2006) The Gibraltar Arc seismogenic zone 20 (part 2): constraints on a shallow east dipping fault plane source for the 1755 Lisbon 21 earthquake provided by tsunami modeling and seismic intensity. Tectonophysics, 2006, vol. 22 426 (1-2), 153 – 166

Harbitz C B (1992) Model simulations of tsunamis generated by the Storegga Slide. Marine Geology 105:1-21

Harbitz C B, Løvholt F, Glimsdal S (2007) Tsunamis Generated by Landslides and Earthquakes – Wave Characteristics and Numerical Modeling for Hazard Assessment in Offshore Geohazards. Proceedings 2007 Offshore Technology Conference, Houston, Texas, 30 April - 3 May 2007. OTC 18602.

Hebert H, Schindele F, Altinok Y, Alpar B, Gazioglu C (2005) Tsunami hazard in the Marmara Sea (Turkey): a numerical approach to discuss active faulting and impact on the Istanbul coastal areas. Marine Geology 215 (1-2):23-43

Heinrich P, Mangeney A, Guibourg S, Roche R (1998) Simulation of water waves generated by a potential debris avalanche in Montserrat Lesser Antilles. Geophys Res Lett 25(9):3697-3700

Heinrich P, Roche R, Mangeney A, Boudon G (1999) Modéliser un raz de marée créé par un volcan. La Recherche 318:67-71

Hornbach MJ, Braudy N, Briggs RW, Cormier M-H, Davis M B, Diebold J B, Dieudonne N, Douilly R, Frohlich C, Gulick S P S, Johnson III H E, Mann P, McHugh C, Ryan-Mishkin K, Prentice C S, Seeber L, Sorlien C C, Steckler M S, Symithe S J, Taylor F W, Templeton J (2010) High tsunami frequency as a result of combined strike-slip faulting and coastal landslides. Nature Geoscience 3, 783–788, doi:10.1038/ngeo975 http://www.nature.com/ngeo/focus/haiti/index.html

Horsburgh K J, Wilson C, Baptie B J, Cooper A, Cresswell D, Musson R M W, Ottemöller L, Richardson S, Sargeant S L (2008) Impact of a Lisbon-type tsunami on the U.K. coastline and the implications for tsunami propagation over broad continental shelves. J. Geophys. Res., vol. 113, C04007, doi:10.1029/2007JC004425

Iida K, Cox D C, Pararas-Carayannis G (1967) Preliminary catalog of tsunamis occurring in the Pacific ocean. Hawaii Institute of Geophysics, Data Report 5:67-10

Intergovernmental Oceanographic Commission (2006) Establishment of an intergovernmental coordination group for tsunami and other coastal hazards warning system for the Caribbean and

adjacent regions UNESCO Resolution XXIII-13 http://ioc3unescoorg/ioc-24/documents/CARIBE-EWS-II-3pdf

ISDR (2009) Global Assessment Report (GAR) on Disaster Risk Reduction http://www.preventionweb.net/gar09/

Komorowski J C, Boudon G, Semet M, Beauducel F, Anténor-Habazac C, Bazin S, Hammouya G (2005) Guadeloupe. In Lindsay J, Robertson R, Shepherd J and Ali S (eds) Volcanic Hazard Atlas of the Lesser Antilles. Seismic Research Unit, the University of the West Indies, Trinidad and Tobago:65-102

Komorowski J C, Boudon G, Semet M P, Villemant B, Hammouya G (2002) Recurrent flank-collapses at Soufrière of Guadeloupe volcano: implications of acid hydrothermal fluids on edifice stability. In Proc Intl Congress "Montagne Pelée 1902-2002" Martinique May 12-16, 2002

Lander J F, Whiteside L S (1997) Caribbean Tsunamis: An Initial History. Tsunami Workshop June 11–13, Mayaguez, Puerto Rico

Le Friant A, Boudon G, Komorowski J C, Heinrich P, Semet M P (2006) Potential flank-collapse of Soufrière volcano Guadeloupe Lesser Antilles? Natural hazards 39(3):381-393

Le Friant A, Hardford C L, Deplus C, Boudon G, Sparks R S J, Herd R A, Komorowski J C (2004) Geomorphological evolution of Montserrat (West Indies): importance of flank collapse and erosional processes. Journal of the Geological Society London 161:147-160

Lindsay J, Robertson R, Shepherd J B, Ali S (eds) (2005) Volcanic Hazard Atlas of the Lesser Antilles. Seismic Research Unit, the University of the West Indies, Trinidad and Tobago

López-Venegas A M, ten Brink U S, Geist E L (2008). Submarine landslide as the source for the October 11, 1918 Mona Passage tsunami: Observations and modelling. Marine Geology 254; 35-46

Løvholt F, Bungum H, Harbitz C B, Glimsdal S, Lindholm C D, Pedersen G (2006) Earthquake related tsunami hazard along the western coast of Thailand. Natural Hazards and Earth System Sciences 6:1-19

Løvholt F, Glimsdal S, Harbitz C B, Zamora N, Nadim F, Peduzzi P, Dao H I, Smebye H (2011) Tsunami hazard and exposure on the global scale. Earth-Science Reviews ISSN 0012-8252 10.1016/j.earscirev.2011.10.002 http://www.sciencedirect.com/science/article/pii/S0012825211001619

Løvholt F, Harbitz C B, Haugen K B (2005) A parametric study of tsunamis generated by submarine slides in the Ormen Lange/Storegga area off western Norway. Marine and Petroleum Geology 22:219-231, doi:101016/jmarpetgeo200410017

Løvholt F, Kühn D, Bungum H, Harbitz C B, Glimsdal S (in review) Historical tsunamis and present tsunami hazard in Eastern Indonesia and the Philippines. Submitted for publication in Journal of Geophysical Research - Solid Earth

Løvholt F, Pedersen G, Bazin S, Kühn D, Bredesen R E, Harbitz C B (in revision) Stochastic analysis of tsunami run-up and dispersion due to heterogeneous co-seismic slip. Accepted for publication in Journal of Geophysical Research - Oceans

Løvholt F, Pedersen G, Gisler G (2008) Oceanic propagation of a potential tsunami from the La Palma Island. Journal of Geophysical Research 113, doi:101029/2007JC004603

Løvholt F, Pedersen G, Glimsdal S (2010) Coupling of dispersive tsunami propagation and shallow water coastal response. In: Zahibo N, Pelinovsky E, Yalciner A, and Titov V (eds): Proceedings of the

"Caribbean Waves 2008" workshop in Guadeloupe Dec 2008. The Open Oceanography Journal, 4, 71-82.

Mader C L (2001) Modeling the La Palma Landslide Tsunami. Science of Tsunami Hazards 19:150-170

Mann P, Calais E, Ruegg J C, DeMets C, Jansma P E, Mattioli G (2002) Oblique collision in the northeastern Caribbean from GPS measurements and geological observations. Tectonics 21(6), doi:101029/2001TC001304

Masson D G, Harbitz C B, Wynn R B, Pedersen G, Løvholt F (2006) Submarine landslides: processes triggers and hazard prediction. Philosophical Transactions of the Royal Society 364, doi:101098/rsta20061810

Maul G A (1993) Climate change in the intra-Americas sea. Edward Arnold London

McCann W R (2006) Estimating the threat of tsunamigenic earthquakes and earthquake induced landslide in the Caribbean. In Mercado-Irizarry A and Liu P (eds) Caribbean Tsunami Hazard. World Scientific Publishing:43-65

Mercado-Irizarry A, Liu P (2006) Caribbean Tsunami Hazard (eds). World Scientific Publishing, 341 pp

Molnar P, Sykes L (1969) Tectonics of the Caribbean and Middle America regions form focal mechanisms and seismicity. Geol Soc Amer Buill 80:1639-1684

Moya J C, Mercado A (2006) Geomorphologic and stratigraphic investigations on historic and prehistoric tsunami in northwestern Puerto Rico: Implications for Long Term Coastal Evolution. In Mercado-Irizarry A and Liu P (eds). Caribbean Tsunami Hazard. World Scientific Publishing:149-177

Müller R D, Roest W R, Royer J-Y, Gahagan L M, Sclater J G (1997) Digital isochrons of the world's ocean floor. Journal of Geophysical Research 102(B2):3211–3214, doi:10.1029/96JB01781

Nadim F, Glade T (2006) On tsunami risk assessment for the west coast of Thailand. Nadim F, Pöttler R, Einstein H, Klapperich H, Kramer S (eds), ECI Symposium Series 7 http://services.bepress.com/eci/geohazards/28

NGI (2009a) Natural Disaster Mitigation in the Caribbean; Local Tsunami Risk Assessment – The Bridgetown Demonstration Project, Norwegian Geotechnical Institute, report 20061575-3

NGI (2009b) Natural Disaster Mitigation in the Caribbean; Scenarios for Earthquake Induced Tsunamis. NORSAR July 2007, Norwegian Geotechnical Institute, report 20061575-4

NGI (2009c) Natural Disaster Mitigation in the Caribbean; Regional Tsunami Exposure Assessment. Norwegian Geotechnical Institute, report 20061575-1

Nikolkina I, Zahibo N, Pelinovsky E (2010) Tsunami in Guadeloupe (Caribbean Sea). In: Zahibo N, Pelinovsky E, Yalciner A, and Titov V (eds): Proceedings of the "Caribbean Waves 2008" workshop in Guadeloupe Dec 2008. The Open Oceanography Journal, 4, 44-49.

NOAA (2008) Tide and currents. http://tidesandcurrents.noaa.gov/ (Accessed December 2008 and November 2011)

NOAA/NGDC (2008) The National Geophysical Data Center tsunami run-up database, www.ngdc.noaa.gov/hazard/tsu.html (Accessed March 1 2008 and November 11 2011)

NTL (2002) Expert Tsunami Database for the Atlantics. Version 36 of March 15 2002, Tsunami Laboratory, Novosibirsk, Russia http://tsun.sscc.ru/htdbwld/

Okada Y (1985) Surface deformation due to shear and tensile faults ina half-space. Bull Seism Soc of Am 74(4) 1135-1154

O'Loughlin KF, Lander JF (2003) Caribbean tsunamis, A 500-year history from 1498-1998. Second edition Springer, The Netherlands, 261 pp

Panagiotopoulos D G (1995) Long-term earthquake prediction in Central America and Caribbean Sea based on the time- and magnitude-predictable model. Bull Seism Soc Amer 85:1190-1201

Pararas-Carayannis G (2002) Evaluation of the threat of mega tsunami generation from postulated massive slope failures of island stratovolcanoes on La Palma, Canary Islands, and on the island of Hawaii. Science of Tsunami Hazards 20(5):251-277

Pararas-Carayannis G (2004) Volcanic tsunami generating source mechanisms in the Eastern Caribbean region. Science of Tsunami Hazards 22(2):74-114

Parry M L, Canziani O F, Palutikof J P (2007) Climate change 2007: impacts adaptation and vulnerability. Contribution of working group II to the fourth assessment report of the intergovernmental panel on climate change. Cambridge University Press, Cambridge

Parsons T, Geist E (2009) Tsunami probability in the Caribbean Region. Pure and Applied Geophysics 165:2089-2116

Pedersen G (2001) A note on tsunami generation by earthquakes. Preprint Series in Applied Mathematics 4, Dept of Mathematics, University of Oslo, Norway

Pedersen G, Løvholt F (2008) Documentation of a global Boussinesq solver. Preprint Series in Applied Mathematics 1, Dept of Mathematics, University of Oslo, Norway http://www.math.uio.no/eprint/appl_math/2008/appl_2008.html

Pelinovsky E, Zahibo N, Dunkley P, Edmonds M, Herd R, Talipova T, Kozelkov A, Nikolkina A (2004) Tsunami generated by the volcano eruption on July 12-13 2003 at Montserrat Lesser Antilles. Science of Tsunami Hazards 22(1):44-57

Poisson B , Pedreros, R (2010). Numerical modelling of historical landslide-genertaed tsunamis in the French Lesser Antilles. Natural Hazards and Earth System Sciences 10:1281-1292

Rabus B, Eineder M, Roth A, Bamler R (2003) The shuttle radar topography mission- a new class of digital elevation models acquired by spaceborne radar. Photogramm Rem Sens 57:241-262

Roger J, Allgeyer S, Hébert H, Baptista M A, Loevenbruck, A, Schindelé F (2010) The 1755 Lisbon tsunami in Guadeloupe archipelago: Source sensitivity and investigation of resonance effects. In: Zahibo N, Pelinovsky E, Yalciner A, and Titov V (eds): Proceedings of the "Caribbean Waves 2008" workshop in Guadeloupe Dec 2008. The Open Oceanography Journal, 4, 58-70.

Ruff L, Kanamori H (1982) Seismicity and the subduction process. Phys. Earth Planet. Int., 23, 240-252

Scheffers A, Kelletat D (2006) New evidence and datings of Holocene paleo-tsunami events in the Caribbean (Barbados St Martin and Anguilla). In: Mercado-Irizarry A and Liu P (eds),Caribbean Tsunami Hazard, World Scientific Publishing:178-202

Shepherd J B, Lynch L L, Tanner JG (1995) An earthquake catalogue for the Caribbean. Pan-American Institute of Geography and History, 120 pp

Sigurdsson H, Carey S, Wilson D (2006) Debris avalanches formation at Kick'em Jenny submarine volcano. In Mercado-Irizarry A and Liu P (eds) Caribbean Tsunami Hazard. World Scientific Publishing

Soloviev S L, Go C N (1984) A Catalogue of Tsunamis on the Western Shore of the Pacific Ocean. Russ Acad of Sci Moscow, 310 pp

Stein S, Engeln J F, Wiens D A, Fujita K, Speed R C (1982) Subduction seismicity and tectonics in the Lesser Antilles arc. Journal of Geophysical Research 87(B10):8642-8664

Stein R S, Okal E A (2007) Ultralong Period Seismic Study of the December 2004 Indian Ocean Earthquake and Implications for Regional Tectonics and the Subduction Process. Bull. Seism. Soc. Am. 97(1A): 279-295, doi:10.1785/0120050617 http://edokappsrv1:8080/sites/1044/GetFile.aspx?fileId=613676

Tanioka Y, Satake K (1996) Tsunami generation by horizontal displacement of ocean bottom. Geophysical Research Letters 23:861–864

Teeuw R, Rust D, Solana C, Dewdney C, Robertson R (2009) Large coastal landslides and tsunami hazard in the Caribbean. EOS Trans 90(10):81-82

ten Brink U S, Danforth W W, Polloni C, Andrews B, Llanes P, Smith S V, Parker E, Uozumi T (2004) New Seafloor Map of the Puerto Rico Trench Helps Assess Earthquake and Tsunami Hazards. EOS 85(37):349-354

ten Brink U, Geist E L, Andrews B.D. (2006b) Size distribution of submarine landslides and its implication to tsunami hazard in Puerto Rico. Geophysical Research Letters 33 (L11307):4 pp doi:10.1029/2006GL026125

ten Brink U, Geist E L, Lynett P, Andrews B (2006a) Submarine slides north of Puerto Rico and their tsunami potential. In Mercado-Irizarry A and Liu P (eds). Caribbean Tsunami Hazard. World Scientific Publishing: 67-90

ten Brink U, Jaffe B E, Geist E L (2005) Tsunami hazard potential in the Caribbean USGS-Woods Hole Science Center http://woodshole.er.usgs.gov/projects/2921C4X.pdf (Accessed April 30, 2008)

Vanneste M, Harbitz C B, De Blasio F V, Glimsdal S, Mienert J, Elverhøi A (2010) The Hinlopen-Yermak Landslide Arctic Ocean – Geomorphology Slide Dynamics and Tsunami Simulations. In Shipp R C, Weimer P, Posamentier H W (eds): The Importance of Mass-Transport Deposits in Deepwater Settings. SEPM Special Publication 95

Villaseñor A, Engdahl R (2007) Systematic Relocation of Early Instrumental Seismicity: Earthquakes in the International Seismological Summary for 1960–1963. Bulletin of the Seismological Society of America 97(6):1820-1832, doi:101785/0120060118

Wadge G, Shepherd, J B (1984) Segmentation of the Lesser Antilles subduction zone. Earth and Pl Sc Lett 71:297-304

Ward S N, Day S (2001) Cumbre Vieja volcano – Potential collapse and tsunami at La Palma, Canary Islands. Geophysical Research Letters 28(17):3397-3400

Wells D L, Coppersmith K J (1994) New empirical relationships among magnitude rupture length rupture width rupture area and surface displacement. Bull Seis Soc Am 84:974-1002

Wynn R, Masson, D (2003) Canary Islands landslides and tsunami generation: Can we use turbidite deposits to interpret landslide processes. In Locat J, Mienert J (eds): Submarine Mass Movements and Their Consequences. Kluwer Acad., Dordrecht, Netherlands:325- 332

Zahibo N, Pelinovsky E (2001) Evaluation of tsunami risk in Lesser Antilles. Natural Hazards and Earth System Sciences 3:221-231

Zahibo N, Pelinovsky E, Kurkin A, Nikolkina I (2008) Tsunami Hazard for the French West Indies Lesser Antilles. In Krishnamurthy RR, Glavovic BC, Kannen A, Green DR, Ramanathan A Han Z, Tinti S, and Agardy T (eds). Integrated Coastal Zone Management (ICZM) 800 pp ISBN 978-981-05-8948-6

Zahibo N, Pelinovsky E, Yalciner A C, Kurkin A, Koselkov A, Zaitsev A (2003) The 1867 Virgin Island Tsunami. Natural Hazards and Earth System Sciences 3:367-376

Tables

Table 1: Run-up data from the 1867 Virgin Islands tsunami

Location	Latitude (°N)	Longitude (°E)	Distance to source (km)	Max water height[(1)] (m)	Observations [(2)]
St. George's,Grenada	12.01	-61.78	765	1.5	1.44 m recede
Gouyave, Grenada	12.17	-61.73	752	3	6.4 m run-up
Basse Terre, Guadeloupe	16.00	-61.72	429	1	2 m run-up
Deshaies, Guadeloupe	16.32	-61.78	404	**10***	4 m recede
Sainte-Rose, Guadeloupe	16.33	61.70	411	**10**	4 m recede over 150 m distance
St. John's, Antigua	17.19	-62.42	302	2.4	2.88 m inundations
Frederiksted, St. Croix	17.71	-64.88	48	7.6	**8.8** m wave height
Charlotte Amalie, St. Thomas	18.33	-64.92	32	6	7.36 m wave height

(1) Maximum water heights listed by NOAA/NGDC (2008) database. *In 2008, the NOAA/NGDC (2008) database listed 18.3 m maximum water height for Deshaies, it has been corrected since and is now (November 2011) reduced to 10 m.

(2) Observations according to BRGM (2009) after revisiting existing archives.

According to Zahibo et al. (2008), houses were destroyed and the sea receded 100 m at Deshaies, while the sea withdrew 100 m and damaged houses upon return as a 10 m wave at Sainte-Rose.

Table 2: Parameter values for the earthquake scenarios

		Dip-slip [m]		*[km]*		
Location	*Segment*	*Start*	*End*	*Length*	*Width*	M_w
Hispaniola	1	0	6	61	55	
	2	6	6	65	55	
	3	6	0	65	55	
	SUM			191		8.0
Lesser Antilles	1	0	6	59	55	
	2	6	6	58	55	
	3	6	0	58	55	
	SUM			173		8.0

Table 3: Parameter values for the landslide scenarios.

Landslide	*Subaerial landslide*	*Submarine landslide*	*Width [km]*	*Height [km]*	*Length [km]*	*Submarine run-out [km]*	*Volume [km^3]**	*V_{max} [m/s]*
Montserrat	X	-	0.8	0.1	1.6	5.4	0.17	30
Kick'em Jenny	-	X	0.8	0.1	5.6	10	0.6	45
St. Lucia	X	-	0.8	0.2	1.2	18	0.25	40

** The volume of the landslide is larger than the product of width, height, and length owing to the rounding of the slide box.*

Figures

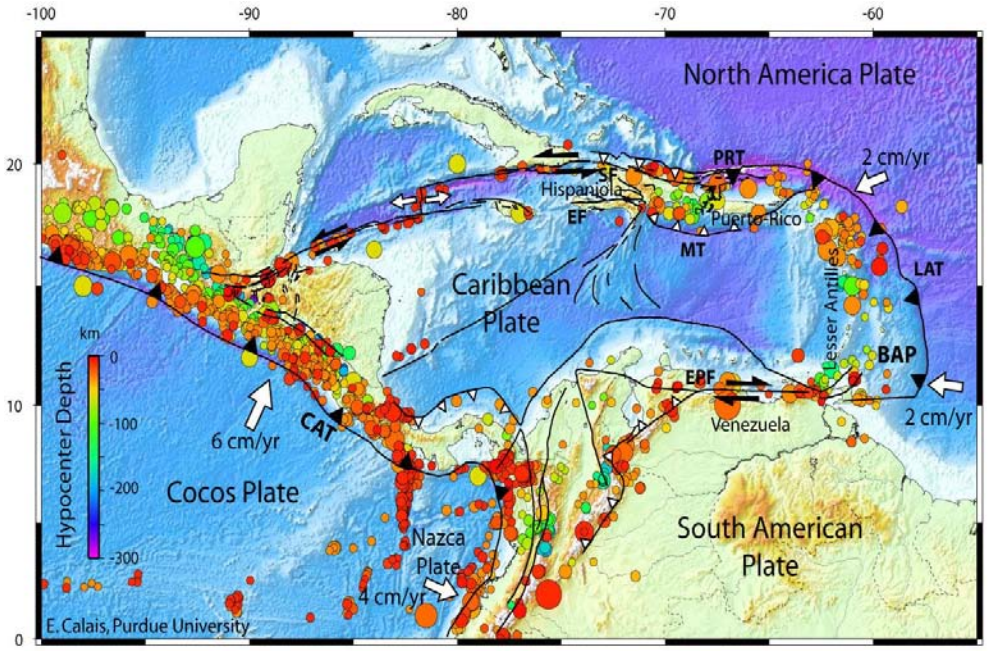

Figure 1: Seismotectonic context of the Caribbean Plate. Seismicity is from USGS/NEIC database (1974-present). This map is modified from E. Calais, http://web.ics.purdue.edu/~ecalais/haiti/. BAP: Barbados Accretionary Prism; CAT: Central American Trench; EF: Enriquillo Fault; EPF: El Pilar Fault; LAT: Lesser Antilles Trench; MT: Muerto Trench; PRT: Puerto Rico Trench; SF: Septentrional Fault. Country names are shown in Figure 2.

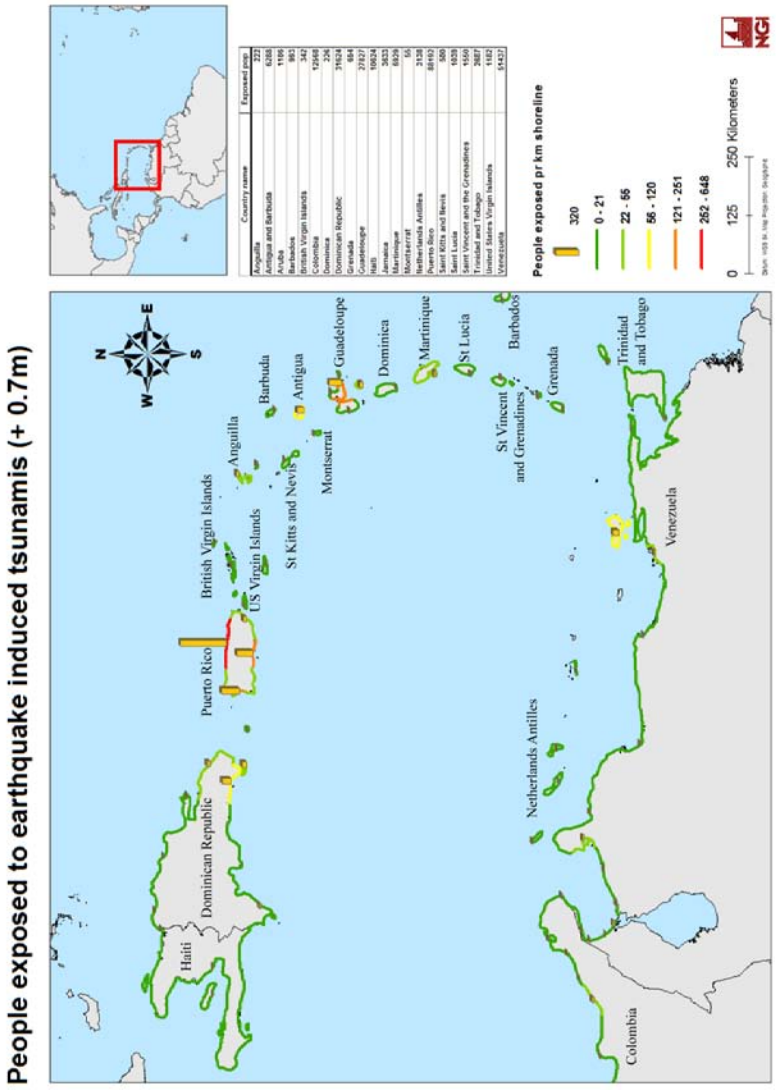

Figure 2: Number of people exposed to earthquake induced tsunami per km shoreline. The bars indicate the exposed population pr km shoreline calculated by defining line segments along the coast with approximately similar population density per unit area. The statistics from these areas are projected into the shoreline for the same area using different colours. The effect of high tide and sea level rise is taken into account. Estimated individual return period is about 500 years.

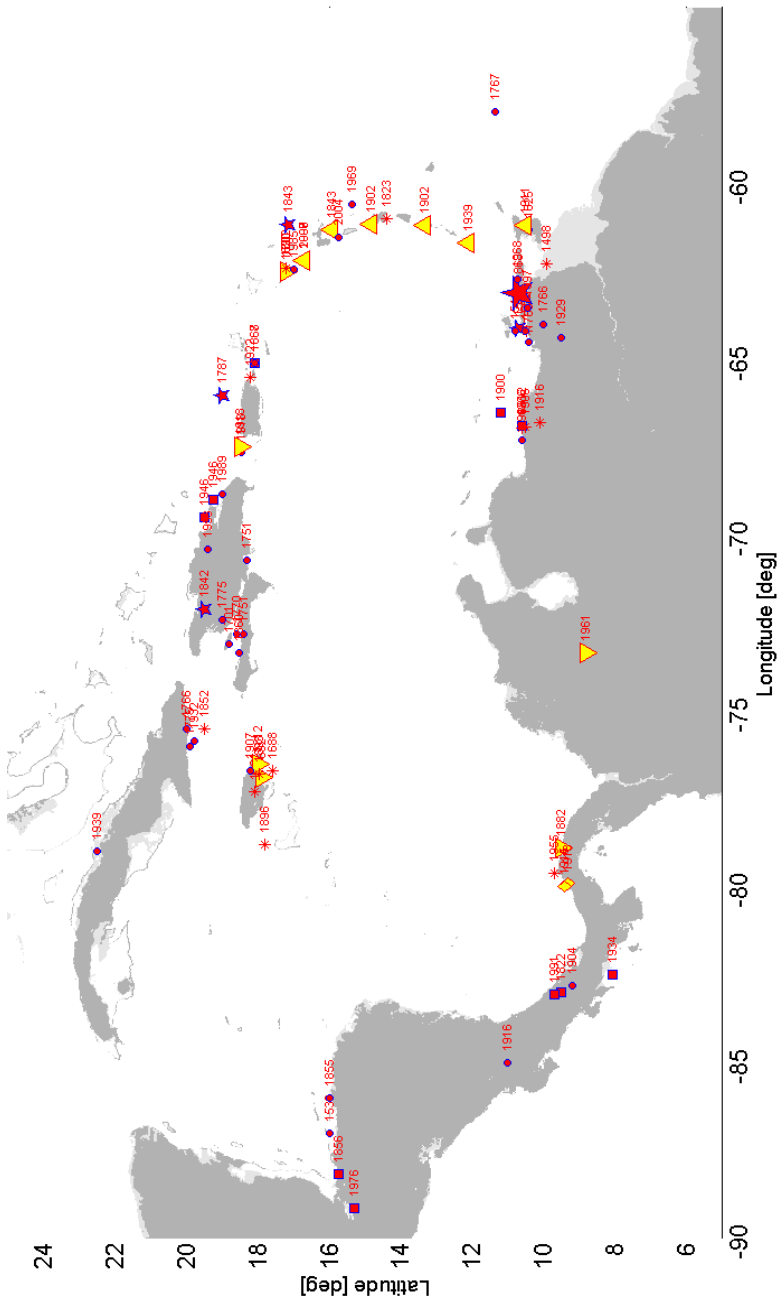

Figure 3: Sources of tsunamis in the Caribbean. We refer to earthquake tsunamis if the tsunamigenic source is categorized in the original data as earthquake or probable earthquake. Red markers represent seismic sources (star means 8.5 > magnitude ≥ 8.0, square means 8.0 > magnitude ≥ 7.5, and circle means magnitude < 7.5), while the yellow upward triangle means volcanic sources, the yellow downward triangle means landslide sources, and yellow rhomboid means combined/unknown/other sources.

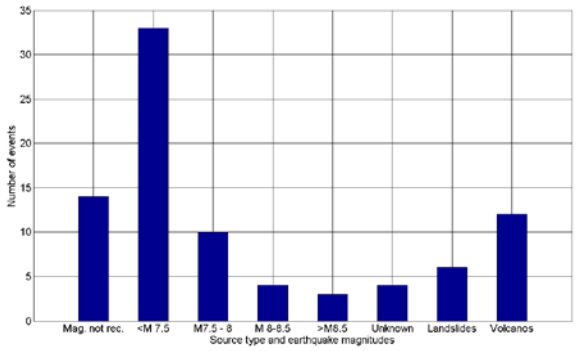
Number of events
Mag. not rec.
<M 7.5
M7.5 - 8
M 8-8.5
>M8.5
Unknown
Landslides
Volcanos
Source type and earthquake magnitudes

(a)

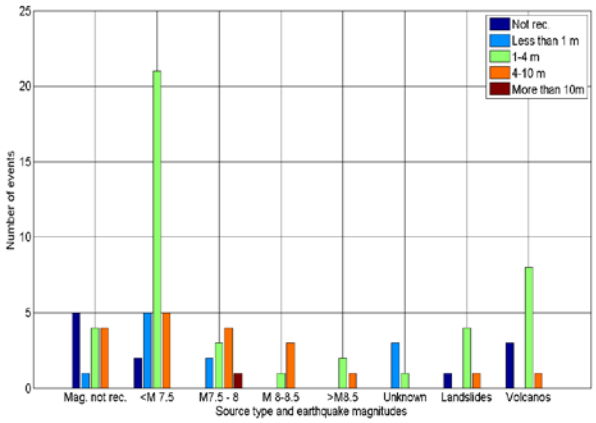
Not rec.
Less than 1 m
1-4 m
4-10 m
More than 10m
Number of events
Mag. not rec.
<M 7.5
M7.5 - 8
M 8-8.5
>M8.5
Unknown
Landslides
Volcanos
Source type and earthquake magnitudes

(b)

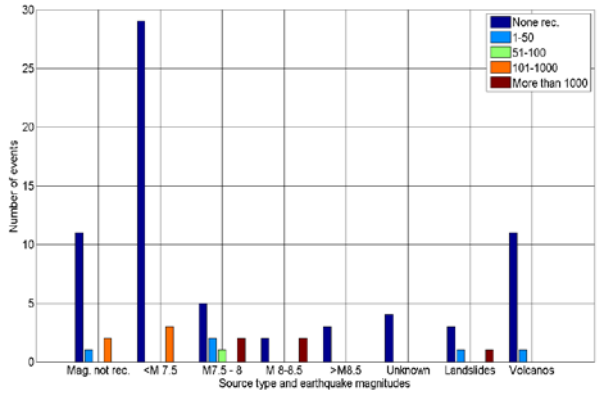
None rec.
1-50
51-100
101-1000
More than 1000
Number of events
Mag. not rec.
<M 7.5
M7.5 - 8
M 8-8.5
>M8.5
Unknown
Landslides
Volcanos
Source type and earthquake magnitudes

(c)

Figure 4: Types of tsunamis in the Caribbean. (a) Number of events with regard to tsunami source type and earthquake source magnitude. M_w is most reliable magnitude estimate and therefore applied when available. (b) Number of events split into ranges of maximum water levels versus tsunami source and earthquake magnitude. (c) Number of events split into ranges of number of fatalities versus tsunami source and earthquake magnitude.

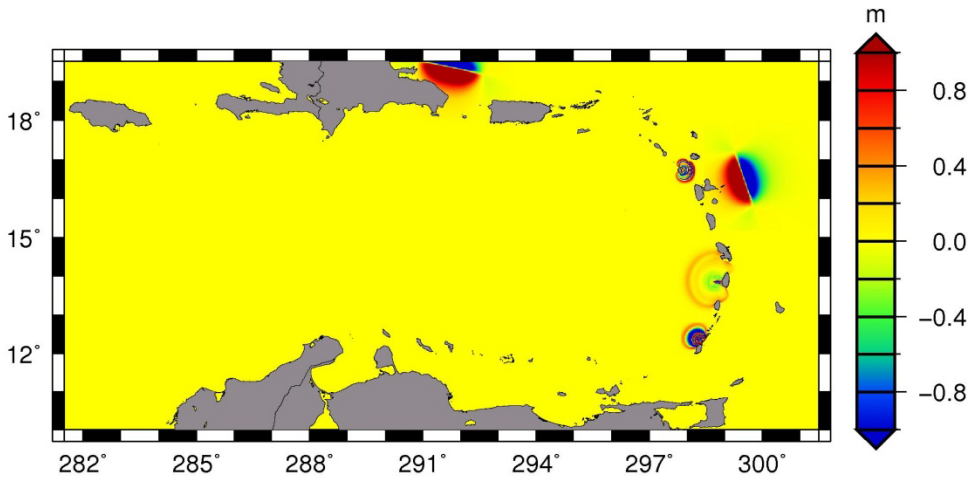

Figure 5: The tsunami surface elevations shortly after the initiation of the five Caribbean scenarios evaluated: two earthquake sources (Hispaniola and Lesser Antilles scenarios) and three landslide sources (Montserrat, St-Lucia and Kick'em Jenny).

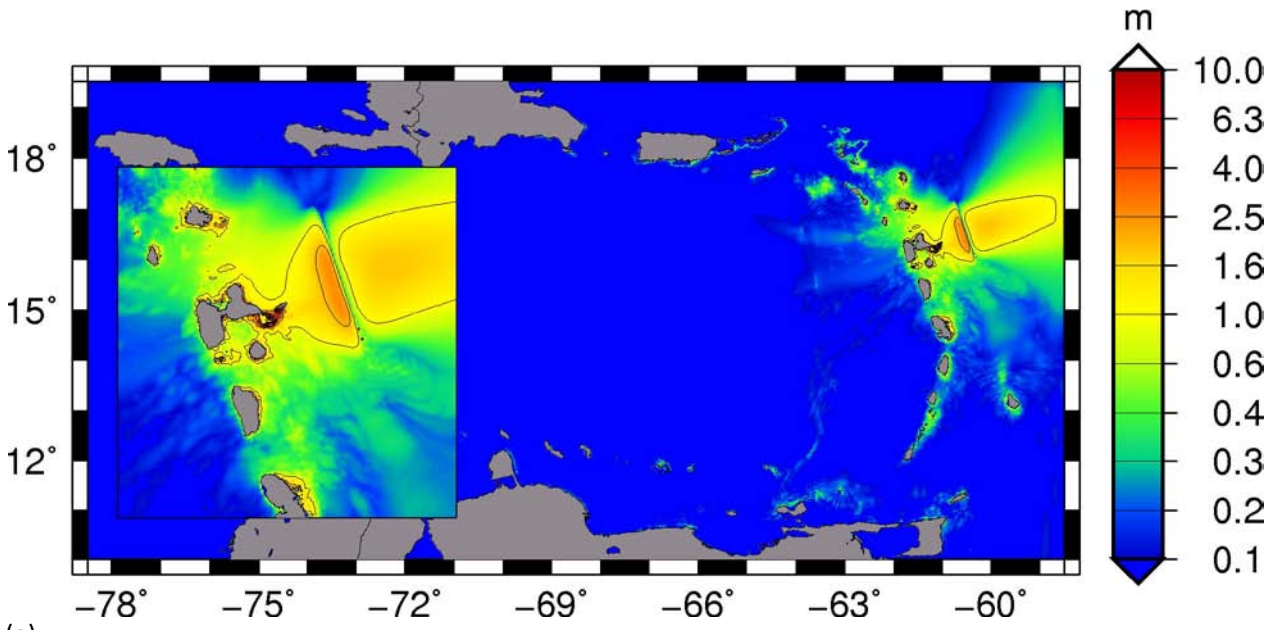

(a)

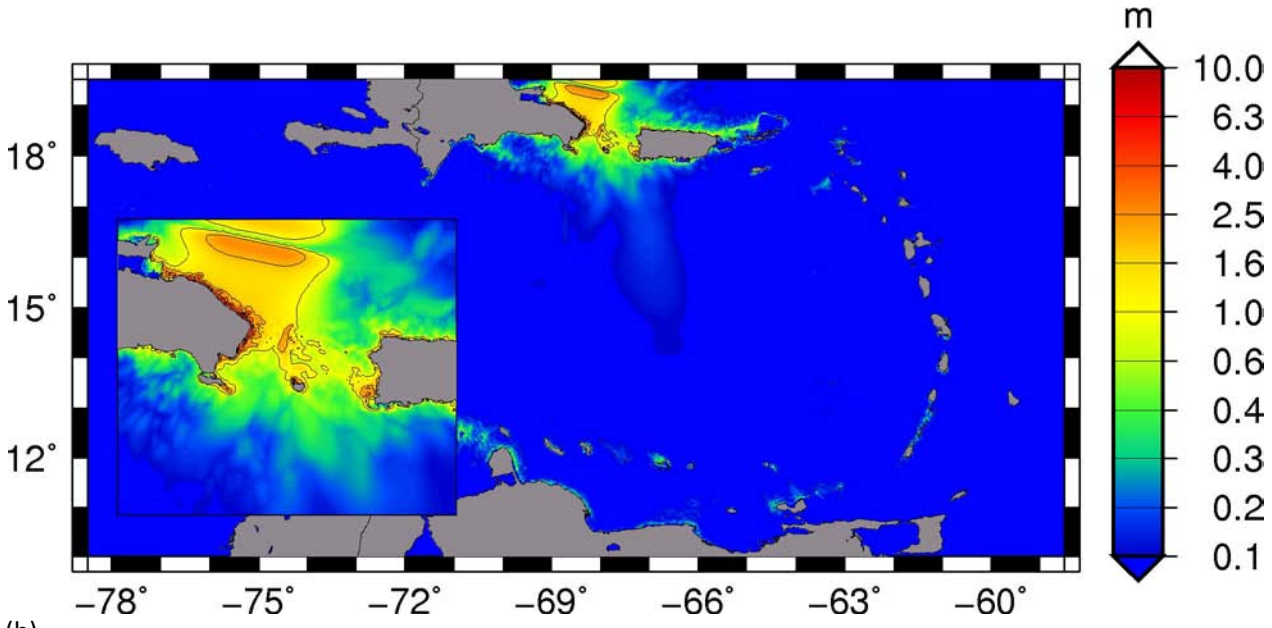

(b)

Figure 6: (a) Maximum surface elevations for the Lesser Antilles earthquake scenario. (b) Maximum surface elevations for the Hispaniola earthquake scenario.

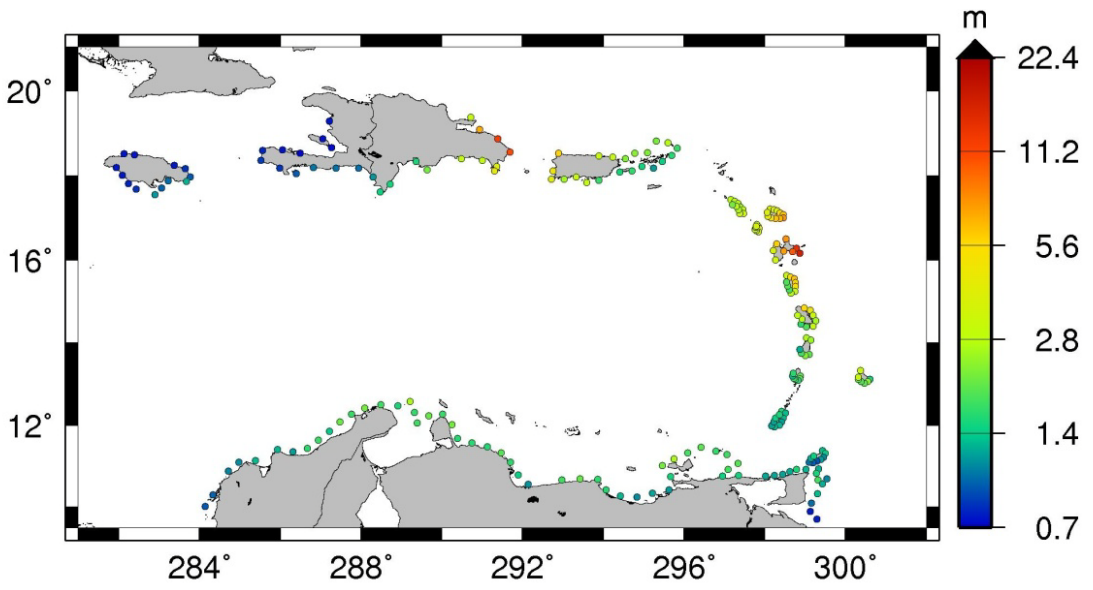

Figure 7: Location of the points where the maximum shoreline water level is calculated with the described procedure. The colours in each point reflects the compilation of the highest estimated maximum water level given in meters for the two potential earthquake tsunami scenarios north of Hispaniola and east of Guadeloupe (Lesser Antilles scenario).

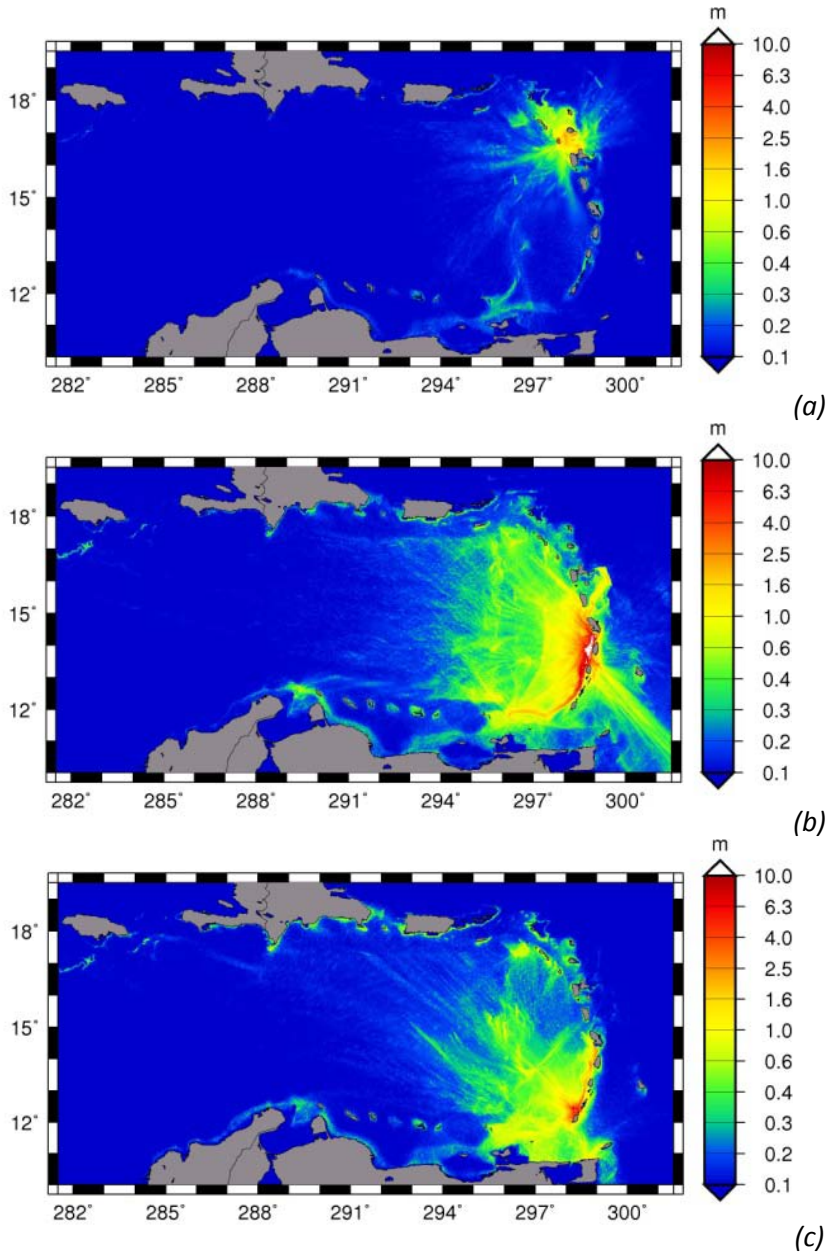

Figure 8: Maximum surface elevations for the three landslide scenarios. (a) flank collapse on Montserrat volcano. (b) dome collapse on St. Lucia volcano. (c) submarine landslide on Kick'em Jenny volcano.

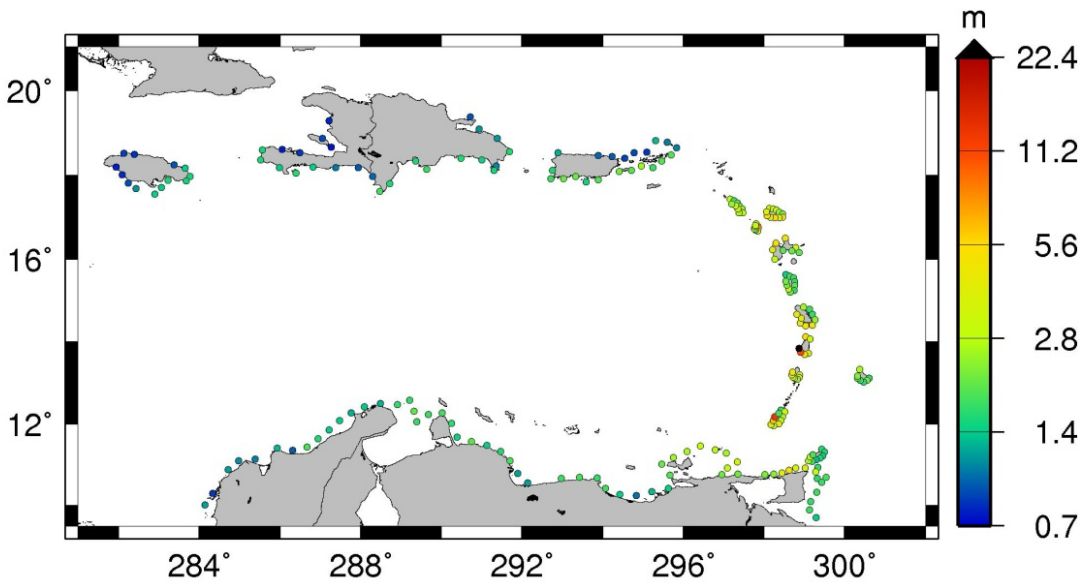

Figure 9: A compilation of the highest estimated maximum water level given in meters for the three landslide scenarios (Montserrat, St Lucia and Kick'em Jenny).

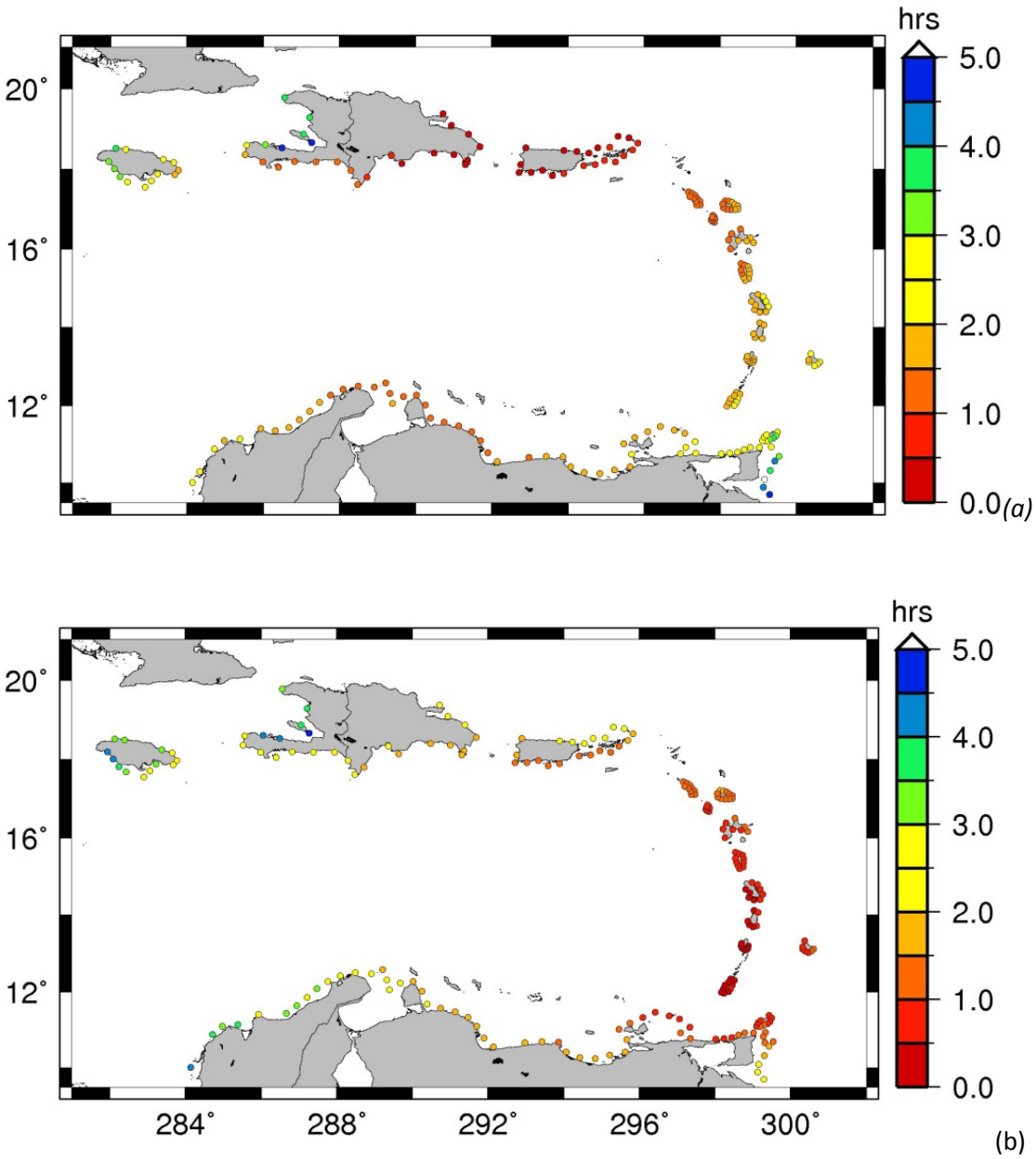

Figure 10: Arrival times (hours) for two selected scenarios: the Hispaniola earthquake (a) and the Kick'em Jenny submarine landslide (b).

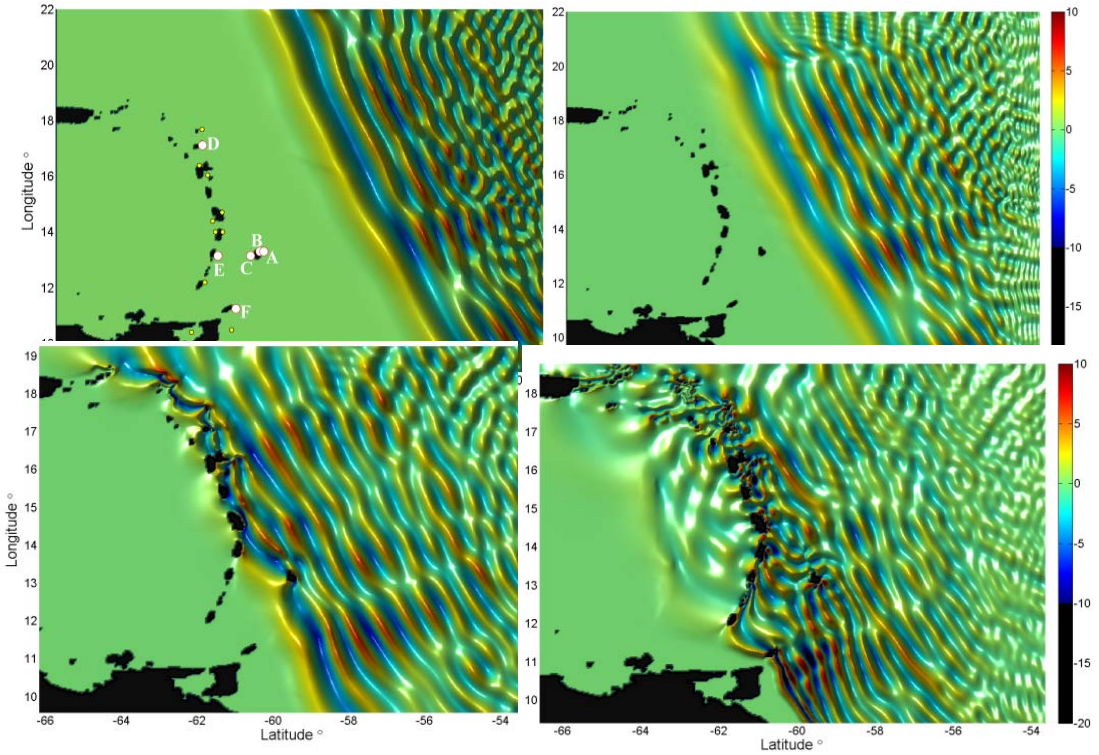

,

a b

c d

Figure 11: Extreme transoceanic tsunami scenario. Snapshots of the simulated surface elevation at 5 h 15 min (a), 5 h 45 min (b), 6 h 15 min (c), and 6 h 45 min (d).

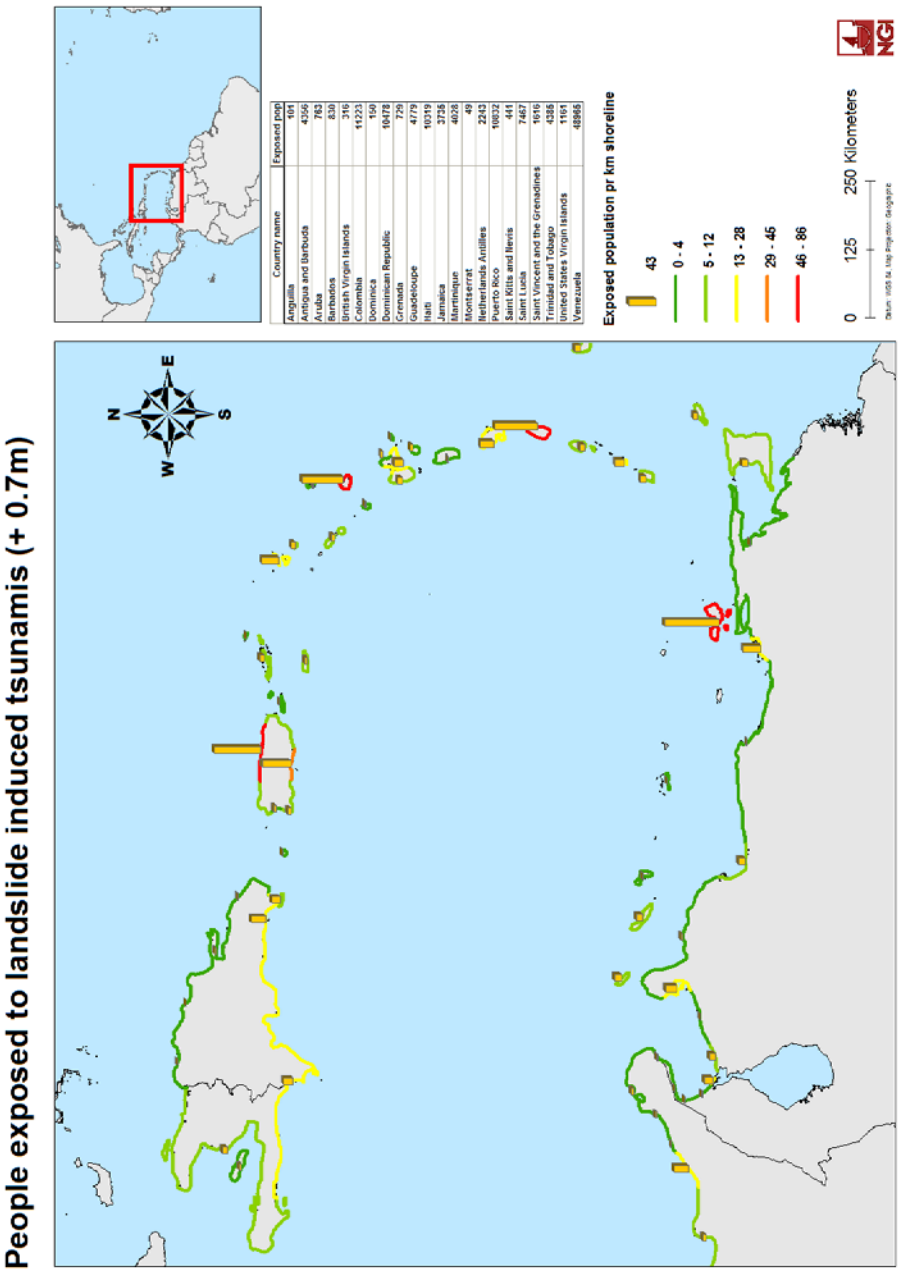

Figure 12: Number of people exposed to landslide induced tsunami per km shoreline. The effect of high tide and sea level rise is taken into account. Estimated individual return period is more than 1000 years for smaller events in the north and about 10 000 years for larger events in the southern part of the arc. Note: different scales of bars and colours compared to Figure 2.

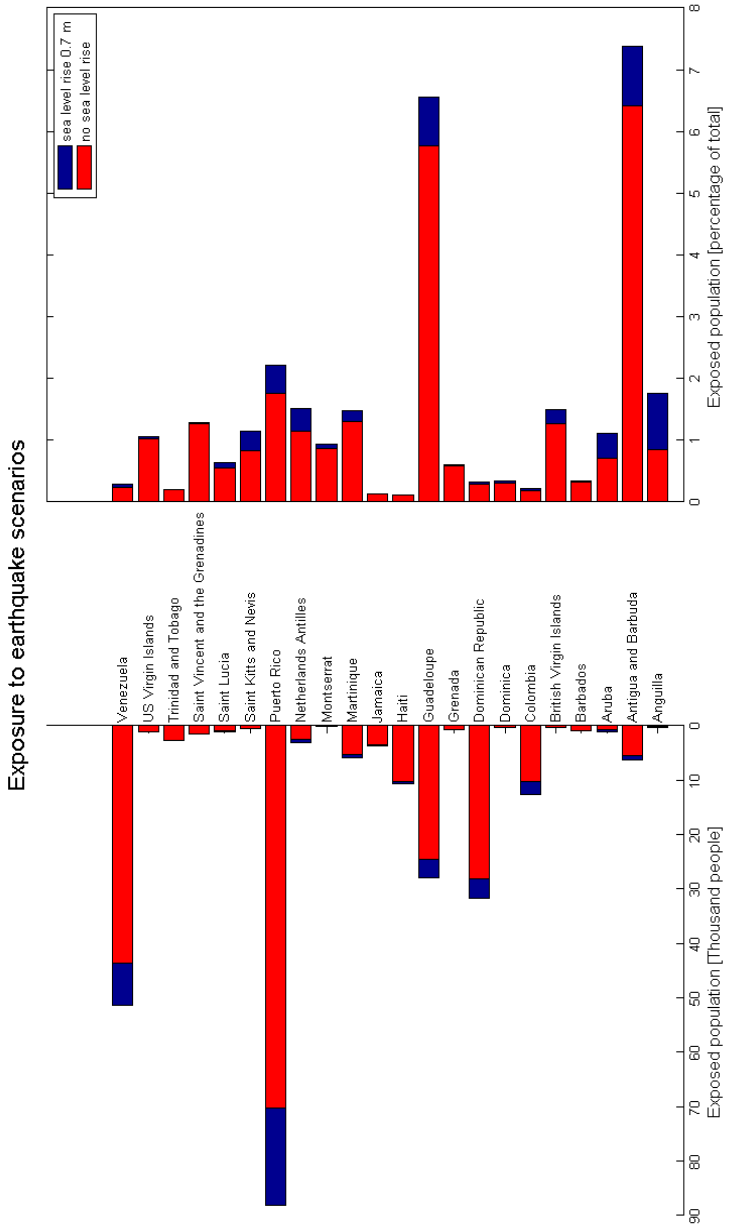

.

Figure 13: Overview of population exposed to earthquake induced tsunamis (estimated individual return period of about 500 years). Left part of the figure shows the total number of people exposed, while the number of exposed people relative to number of inhabitants in each country is shown to the right. The effect of sea level rise is taken into account in blue.

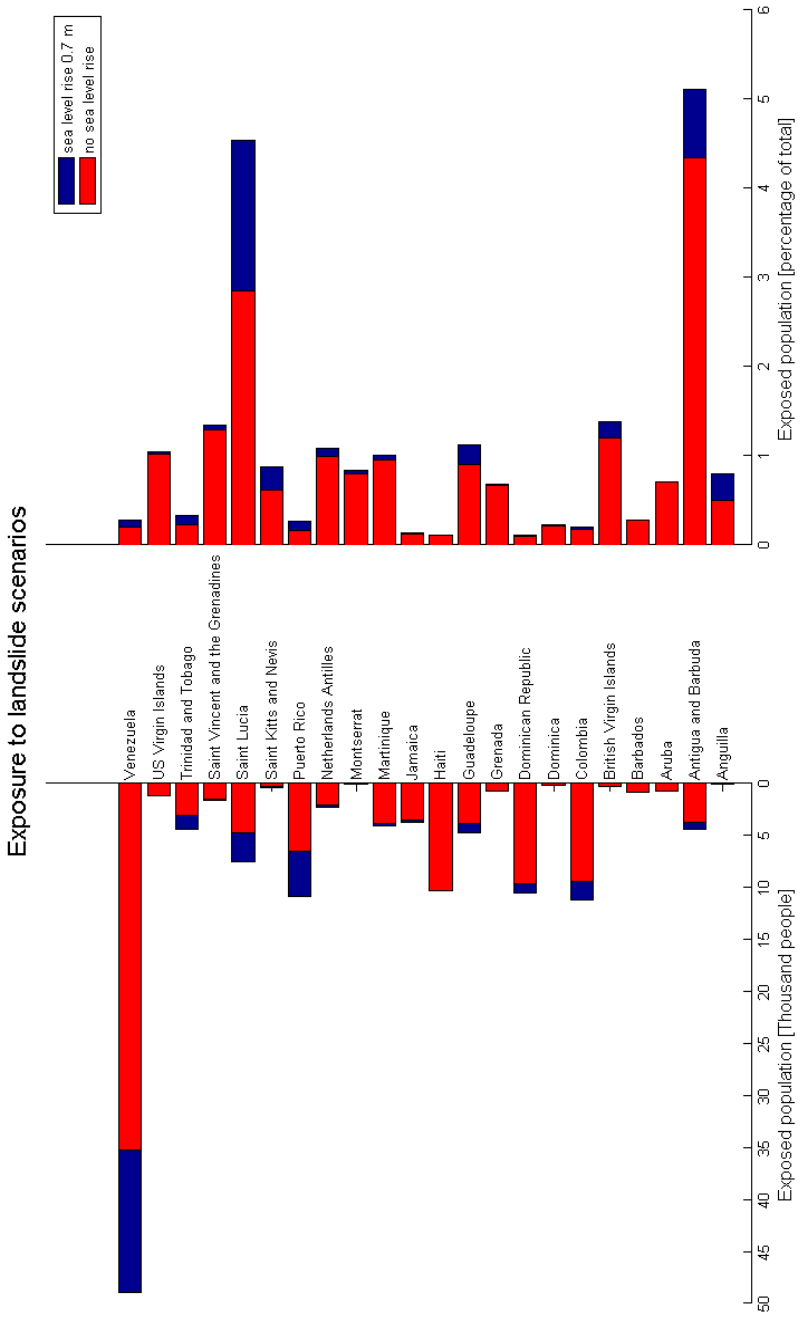

Figure 14: Overview of population exposed to landslide induced tsunamis (estimated individual return period is more than 1000 years for smaller events in the north and about 10 000 years for larger events in the southern part of the arc). Left part of the figure shows the total number of people exposed, while the number of exposed people relative to number of inhabitants in each country is shown to the right. The effect of sea level rise is taken into account in blue.

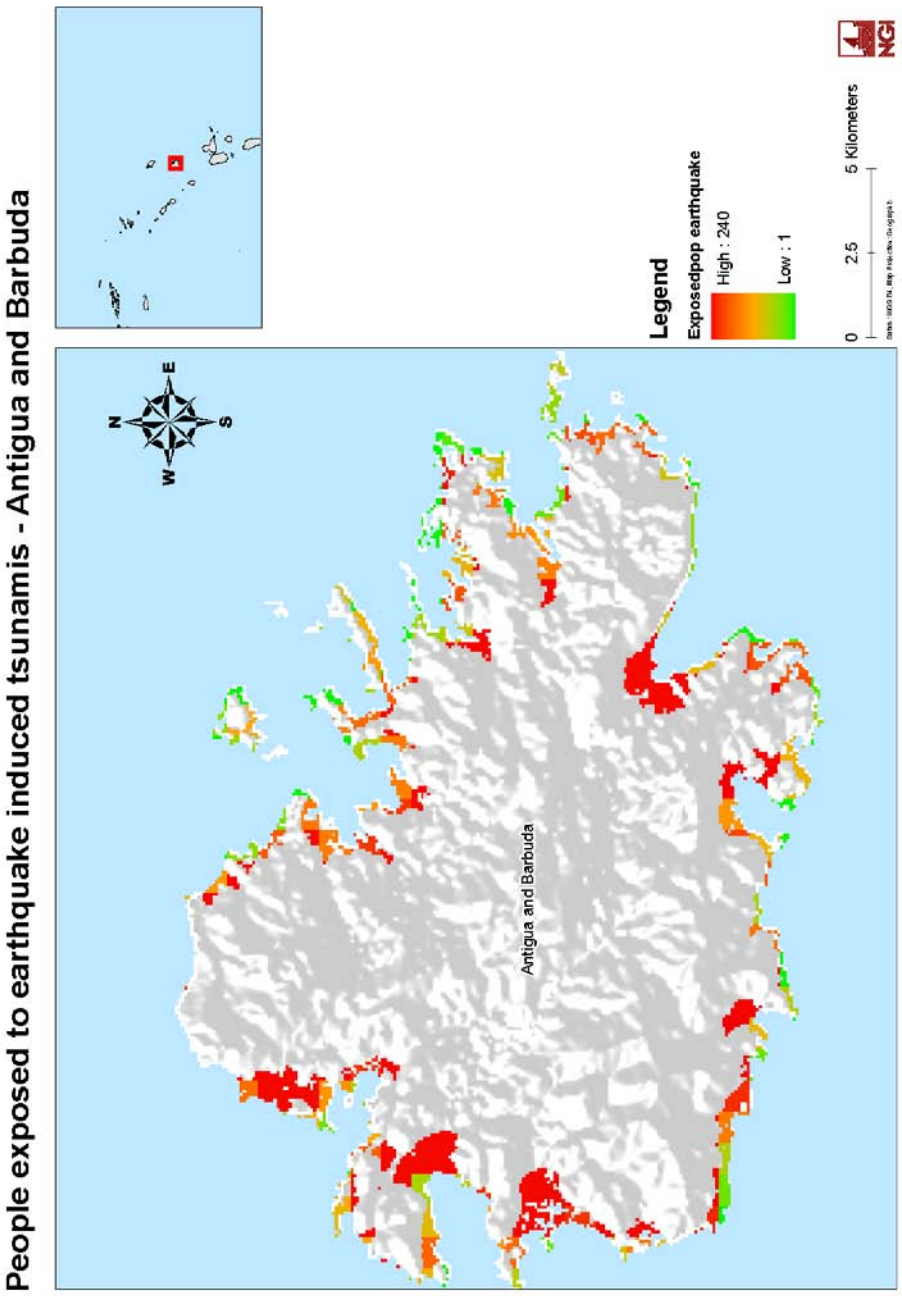

Figure 15: Number of people exposed to earthquake induced tsunamis per 30 arc sec square (0.75 km^2) in Antigua. The effect of high tide and sea level rise is taken into account. Estimated individual return period is about 500 years.

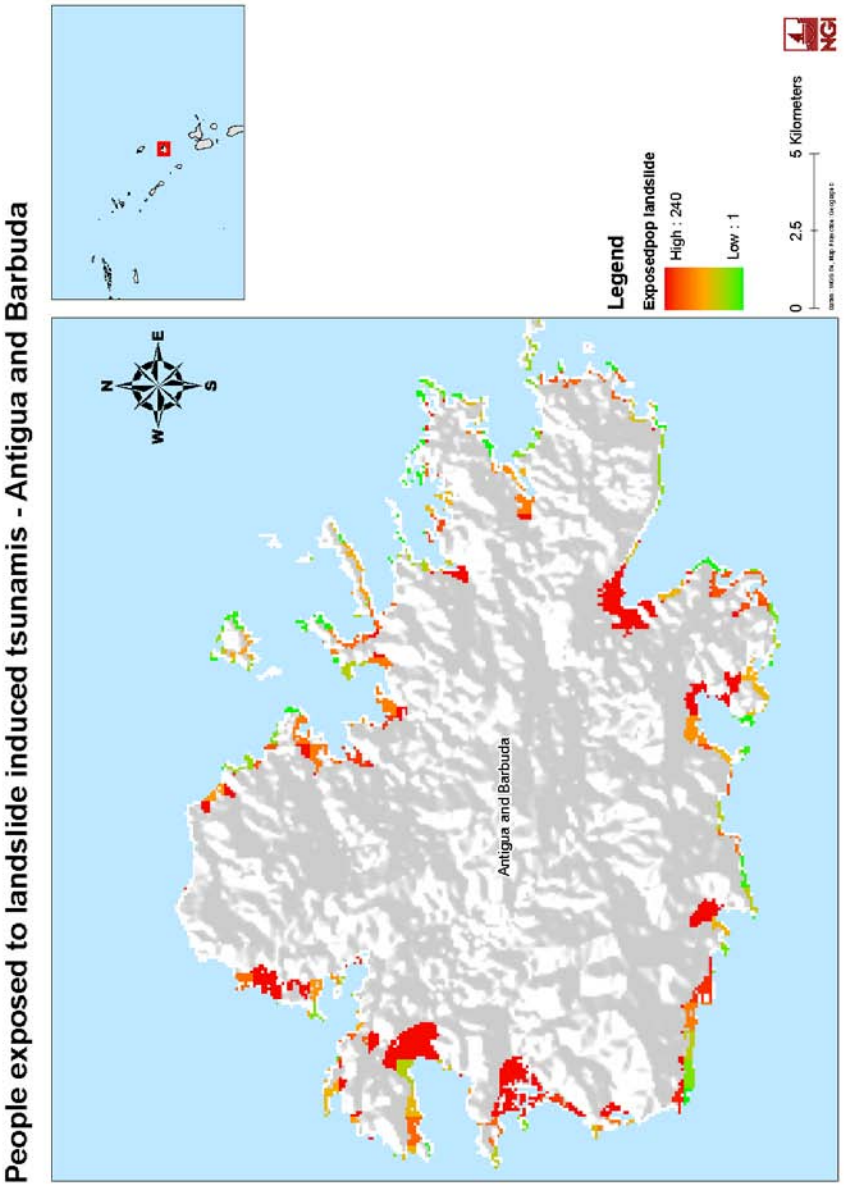

Figure 16: Number of people exposed to landslide induced tsunamis per 30 arc sec square (0.75 km^2) in Antigua. The effect of high tide and sea level rise is taken into account. Estimated individual return period is more than 1000 years for smaller events in the north and about 10 000 years for larger events in the southern part of the arc.

Appendix: The NGI/NORSAR Caribbean tsunami database

Year	Month	Day	Hour	Tsunami cause code	Magnitude type not specified		Magnitude (Ms)		Magnitude (Mw)		Magnitude (Mt - Abe)	Focal Depth (km)	Tsunami event Validity	Country	Region	Lat.	Long.	Magnitude (Lida)	Intensity (Soloviev)	Max. wave height [m]	Number of deaths	Casualty idx.
1498	8	2		1									3	VENEZUELA	BOCA DE LA SIERPE	9,9	-62,3		1			3
1530	9	1	14	1			7		8			10	4	VENEZUELA	CUMANA	10,7	-64,1	2,6	2	7,3		
1539	11	24	23	1			7						3	HONDURAS	CABO DE HIGUERAS	16	-87		1			
1541	12	25		1			7						2	VENEZUELA	CUBAGUA ISLAND	10,8	-64,2		1			
1688	3	1		1									2	Port Royal.	Jamaica	17,6	-76,7		2			
1690	4	5		3	7,6		7						3	Antigua; Nevis, St. Thomas, etc		17,2	-62,5		1	2	2	
1692	6	7	16	3	7,5		7					10	4	JAMAICA	PORT ROYAL	17,9	-76,9		3	1,8	2500	4
1701	11	9		1			7						2	Gon(n)ave.	Haiti	18,8	-73,1		1			
1750				1			7						3	Cumana.	Venezuela	10,4	-64,5		1			
1751	10	18	19	1	7,3		7					33	3	DOMINICAN REPUBLIC	AZUA DE COMPOSTELA	18,3	-70,7		2			
1751	11	21		1			7						3	All	All	18,4	-72,8		2	7		
1755	11	1	9	1			8,5						4	All	All	36	-11	3,6	3,5	6,4		
1755	11	18	9	1			7						3	All	All	42,7	-70,3		4	6,3		
1761	3	31	0	1			8,5				8,5		4	Barbados	Barbados	34,5	-13	1,3	2	1,2		
1766	6	11	24	1			7						2	Jamaica	Jamaica	20	-75,5		2			
1766	10	21		1			7						3	Cumana.	Venezuela	10	-64		1			
1767	4	24	6	1			7						3	Martinique and Barbados	Martinique and Barbados	11,35	-57,95		1	2,8		
1770	6	3	9	1			7					10	4	HAITI	PORT-AU-PRINCE	18,6	-72,8		1		200	
1775	2	11		1			7						3	CUBA	SANTIAGO DE CUBA	19,9	-76		1			
1775	12	18		1			7						3	HAITI	HAITI & DOMINICAN REPUBLIC	19	-72,4		1			
1781	8	1		2									2	JAMAICA	JAMAICA: UNKNOWN LOCATION	18,1	-77,3					
1787	3	28		1			8						4	S. MEXICO	MEXICO	19	-66		2,5	4		
1802	3	19		1									3	Antigua and St. KittsAntigua and St. Kitts	Antigua and St. KittsAntigua and St. Kitts	17,2	-62,4		1			
1802	8	15		1								0	3	VENEZUELA	CUMANA	10,48	-64,2					
1812	3	26	20	1	7,7							33	2	VENEZUELA	LA GUAIRA	10,6	-66,9		2			
1812	11	11	10	3									2	JAMAICA	KINGSTON	18	-76,5		2			
1822	5	7	23	1			7,6						3	COSTA RICA	MATINA	9,5	-83		1			
1823	11	30	3	1									4	MARTINIQUE	SAINT PIERRE	14,4	-61		2			
1825	9	20	4	1			7						2	TRINIDAD AND TOBAGO	PORT-OF-SPAIN	10,4	-61,3		1			
1842	5	7	21	1	8,05		8,1						4	HAITI	Port de Paix	19,5	-72,1	4,2	3	4,6	4500,00	3
1843	2	8	14	1	8		8,3					33	4	Antigua	St John	17,15	-61,17	0,3	1	1,2	5000	
1843	2	17		6									2	Guadeloupe	Marie-Galante	15,93	-61,3		0			
1852	7	17		1									2	CUBA	SANTIAGO DE CUBA	19,5	-75,5		2			
1853	7	15	14	1	6,7		6,7					14	4	VENEZUELA	CUMANA	10,5	-64,2		1			3
1855	9	25	10	1			6,5						2	Honduras. Trujillo Bay		16	-86		1			
1856	8	9		1	7,5							0	4	HONDURAS	OMOA	15,75	-88,17		2	5		
1860	4	8	10	1	7,5		7						4	HAITI	ANSE-A-VEAU	18,52	-73,35		1			
1867	11	18	18	1	7,5		7,5					33	4	all	all	18,1	-65,1	2,3	3	9	30	1
1868	3	17	6	1			7						4	USA TERRITORY	VIRGIN ISLANDS	18,1	-65,1	-0,7	1	1,5		
1868	8	13		1	8,5								3	VENEZUELA	RIO CARIBE	10,7	-63,1		1			
1882	9	7	7	3	7,9		7,9						4	PANAMA	SAN BLAS ARCHIPELAGO	9,5	-78,9		1,5	3	100	2
1893	2	19	1	1									2	JAMAICA	KINGSTON	17,97	-76,8		1			
1896	2	6	13	1									2	Kingston. Jamaica		17,8	-78,8		1			
1900	10	29	4	1	7,7	MsAN2	7,6	P&S	7,7	P&S		60	3	VENEZUELA	MANCUTO	11,2	-66,5		3	10		4
1902	5	5	13	7									4	MARTINIQUE	Saint-Pierre	14,82	-61,17		2	2		
1902	5	7		6									4	Barbados, Grenada, Saint Lucia	Barbados, Grenada, Saint Lucia	13,33	-61,18			1		
1902	5	8	8	6									3	MARTINIQUE	Saint-Pierre	14,82	-61,17					
1902	5	20		6									2	MARTINIQUE	Basse-Pointe,Le Prêcheur, Fort de France, Le Carbet	14,82	-61,17				2	
1902	8	30	21	6									3	MARTINIQUE	Fort-de-France	14,82	-61,17		0	1		
1904	12	20	5	1	7,8	G&R	7,2	AN2	7,2	P&S			2	Panama. Costa Rica		9,2	-82,8					
1906	1	31		1									2	VENEZUELA	CARACAS	10,5	-66,916				500	
1906	2	16		1									2	VENEZUELA	Cabo Blanca	10,6	-66,95					
1907	1	14	21	1	6,5	GAN							3	JAMAICA	JAMAICA	18,2	-76,7	1,3	2	2,5	1000	
1911	11	3		6									4	TRINIDAD AND TOBAGO	TRINIDAD	10,5	-61,2		1			
1913	10	2		0									2	Gatun. Panama		9,3	-79,9		-2	0,03		
1914	5	28		0									2	Gatum. Panama		9,4	-80		-1	0,15		
1915	11	26		0									2	Gatun. Panama		9,4	-80		-2	0,01		
1916	4	26	2	1	7,3	G&R	7,4	AN1	7,2	P&S		0	4	PANAMA	BOCAS DEL TORO	11	-85		1	1,2		
1916	7	30		1								0	2	VENEZUELA	OCUMARE DE LA COSTA DE ORO	10,1	-66,8					
1918	10	11	14	1	7,5	MsABE1	7,3	P&S	7,3	P&S		60	4	USA TERRITORY	PUERTO RICO: MONA PASSAGE	18,473	-67,631	2,6	2,5	6,1	142	3
1918	10	24	3	3									4	USA TERRITORY	PUERTO RICO	18,5	-67,5					
1922	5	2	20	1									2	USA TERRITORY	PUERTO RICO: VIEQUES	18,2	-65,5		0	0,64		
1929	1	17	11	1	6,9	G&R						35	4	VENEZUELA	CUMANA	9,499	-64,381		1			
1932	2	3	6	1	6,8	G&R						25	4	CUBA	SANTIAGO DE CUBA	19,77	-75,85		1			
1934	7	18	1	1	7,6	MsABE1	7,4	P&S	7,6	P&S		25	4	Panama. Puerto Armueles		8,045	-82,48			1,3		
1939	7	24		4									2	Grenada		12,1	-61,7					
1939	8	15	3	1	5,6	G&R							2	CUBA	SANTA CLARA	22,5	-79		1			
1946	8	4	17	1	8,1	G&R	8	ABE1	7,9	P&S		60	4	DOMINICAN REPUBLIC	NORTHEASTERN COAST	19,25	-69	2,2	2	5	1790	4
1946	8	8	13	1	7,6	G&R	7,6	ABE1	7,5	P&S		25	4	DOMINICAN REPUBLIC	NORTHEASTERN COAST	19,5	-69,5		0	0,6	75	2
1953	5	31	19	1	6,9	ROTHE	6,8	PAS				33	2	DOMINICAN REPUBLIC	PUERTO PLATA	19,4	-70,4	-3,3	0,5	0,6		
1955	1	18		1								33	2	PANAMA	PANAMA: OFF NORTHERN COAST	9,7	-79,6		2		0	
1961	6	16	10	8	6	PAS						114,9	2	COLOMBIA	NORTHEASTERN COLOMBIA	8,824	-73,337		1			
1967	7	29	23	1			6,5					10	2	VENEZUELA	CARACAS	10,6	-67,3		-1	0,07		
1968	9	20	6	1	6,2	mbGS	6,2	ISC				102,6	2	VENEZUELA	CARUPANO	10,731	-62,719					
1969	12	25	21	1	7	MsABE1	7	P&S	7,2	P&S		9,7	4	Barbados	Barbados	15,37	-60,58	-3,3	0	0,46		
1976	2	4	9	1	7,7	MwP&S	7,5	P&S	7,5	HRV		12,1	4	Guatemala. Gulf of Honduras		15,297	-89,145		0	0,45		
1985	3	16	14	1	6,5	MwGS	6,4	ISC	6,4			15,8	4	GUADELOUPE	Basse-Terre	16,982	-62,446	-3,3	-2	0,03		
1989	11	1	10	1	5,2	mbISC	4,4	ISC				18	3	USA TERRITORY	PUERTO RICO	19	-68,83		-1	0,1		
1991	4	22	21	1	7,3	MwGS	7,5	ISC	7,6	HRV		12,3	4	COSTA RICA	LIMON, PANDORA	9,675	-83,072	1	1,5	3	2	1
1997	4	10		0									2	Honduras								
1997	7	9	19	1	6,9	MwGS	6,8	ISC	7	HRV		10	3	VENEZUELA	CARIACO-CUMANA	10,448	-63,533		1			
1997	12	26	8	7								0	4	MONTSERRAT	WHITE RIVER VALLEY	16,72	-62,18		1	3		
1999	1	20		6									4	MONTSERRAT	SOUFRIERE HILLS VOLCANO	16,72	-62,18			2		
2003	7	13	3	6									4	MONTSERRAT	SOUFRIERE HILLS VOLCANO	16,72	-62,18		0	4		
2004	11	21	11	1	6,3	MwGS	6,1	GS	6,3	HRV		14	4	GUADELOUPE	Les Saintes	15,75	-61,53			2		
2006	5	20	7	6									4	Guadeloupe	Deshaies	16,72	-62,18			1		

From NOAA :

Tsunami Event Validity:
Valid values: **0 to 4**
Validity of the actual tsunami occurrence is indicated by a numerical rating of the reports of that event:

0 = erroneous entry
1 = very doubtful tsunami
2 = questionable tsunami
3 = probable tsunami
4 = definite tsunami

Description of Number of Deaths from the Tsunami:
Valid values: **0** to **4**
When a description was found in the historical literature instead of an actual number of deaths, this value was coded and listed in the **Deaths D** column.
If the actual number of deaths was listed, a descriptor was also added for search purposes.

0 = None
1 = Few (~1 to 50 deaths)
2 = Some (~51 to 100 deaths)
3 = Many (~101 to 1000 deaths)
4 = Very many (over 1000 deaths)

Tsunami Cause Code:
Valid values: **0 to 11**
The source of the tsunami:

0 = Unknown Cause
1 = Earthquake
2 = Questionable Earthquake
3 = Earthquake and Landslide
4 = Volcano and Earthquake
5 = Volcano, Earthquake, and Landslide
6 = Volcano
7 = Volcano and Landslide
8 = Landslide
9 = Meteorological
10 = Explosion
11 = Astronomical Tide

Magnitude (Lida) = log2(H)
Intensity (Soloview) = log2(H/sqrt(2))

Abbreviations:
NOAA - National Geophysical Data Centre, NOAA/WDC Historical Tsunami Database at NGDC, http://www.ngdc.noaa.gov/hazard/tsu_db.shtml
TLN - Historical Tsunami Database for the World Ocean (HTDBWLD), Tsunami Laboratory, Novosibirsk, http://tsun.sscc.ru/On_line_Cat.htm

EHB - Engdahl, E.R., R van der Hilst and R. Buland (1998): Global teleseismic earthquake relocation with improved travel times and procedures for depth determination. Bull. Seism. Soc. Am., 88, 722-743.
- Engdahl, E.R. and A. Villasenor (2002): Global Seismicity: 1900-1999. International Handbook of Earthquake and Engineering Seismology, Volume 81A, pp. 665-690. Published by IASPEI, Committee of Education.
- Engdahl, E.R., A. Villasenor, H.R. DeShon, and C.H. Thurber (2007): Teleseismic Relocation and Assessment of Seismicity (1918–2005) in the Region of the 2004 Mw 9.0 Sumatra–Andaman and 2005 Mw 8.6 Nias Island Great Earthquakes. Bull. Seism. Soc. Am., V
- Bilek, S.L., and E.R. Engdahl (2007), Rupture characterization and aftershock relocations for the 1994 and 2006 tsunami earthquakes in the Java subduction zone, Geophys. Res. Lett., 34, L20311, doi:10.1029/ 2007GL031357.
- Villaseñor, A. and E.R. Engdahl (2007): Systematic Relocation of Early Instrumental Seismicity: Earthquakes in the International Seismological Summary for 1960–1963. Bull. Seism. Soc. Am., Vol. 97, No. 6, pp. 1820–1832, December 2007.
+ personal communication (data files)

GS - USGS (earthquake locations reported under different acronyms over the years, including NEIC, NElS and C&GS, NOAA, NGDC and PDE - Prelimary Determination of Epicenters)
ABE - Catalog of large earthquakes, mostly magnitude 6.8 and larger, 1897-1980, from Abe (1981, 1984) and Abe and Noguchi (1983a,b). The magnitude sources ANI, AN2, ABEl and ABE2 are from this catalog
B&D - Catalog of large earthquakes, 1897-1977, compiled by Bath and Duda (1979)
G&R - Catalog of hypocenters and magnitudes, 1904-1952 (Gutenberg and Richter, 1954)
ISC - Hypocenters and magnitudes from bulletins prepared by the International Seismological Centre, Newbury, UK, 1964-
ISS - Hypocenters listed in the Intemational Seismological Summary (predecessor of ISC), 1918-1963
P&S - Complete and uniform catalog of worldwide earthquakes with Ms magnitudes of 7.0 and larger at depths less than or equal to 70km, 1900-1989 (Pacheco and Sykes, 1992)
PAS - Magnitudes reported by the Califomia Institute of Technology, Pasadena, USA